PYRUVATE CARBOXYLASE EXPRESSION MODULATES PRIMARY MAMMARY TUMOR GROWTH AND CENTRAL CARBON METABOLISM

Alexander J. Pfeil

A thesis submitted to the faculty at the University of North Carolina at Chapel Hill in partial fulfillment of the requirements for the degree of Master of Science in the Department of Nutrition in the Gillings School of Global Public Health.

Chapel Hill
2022

Approved by:

Stephen D. Hursting

Justin J. Milner

Michael K. Wendt

ABSTRACT

Alexander J. Pfeil: Pyruvate Carboxylase Expression Modulates Primary Mammary Tumor Growth and Central Carbon Metabolism
(Under the direction of Stephen D. Hursting)

Metabolic reprogramming is a fundamental requirement for triple-negative breast cancer's (TNBC) growth and progression, with pyruvate carboxylase (PC) identified as a key mediator of breast cancer metastasis to the lung. Less is known, however, of PC's role at the primary site. This study thus aimed to investigate the impact of PC suppression on primary tumor growth and if PC expression could inform the use of targeted metabolic therapies to augment currently used treatments for TNBC. Two separate PC knockdown cell lines revealed PC suppression to drive both a pro-tumor and anti-tumor effect, revealing a complex relationship between PC expression and tumor growth. PC suppressed M-Wnt cells in culture produced more lactate and had reduced rates of oxidative phosphorylation, rendering them more sensitive to lactate metabolism inhibition. This study highlights a dichotomous role for PC at the primary site that warrants additional investigation into utilizing PC to inform metabolic-based therapies.

ACKNOWLEDGMENTS

This project would not have been possible without the constant support of Dr. Hursting and the encouraging, rigorous, and curious lab environment that he has fostered. I would like to thank Dr. Hursting for giving me the opportunity to begin my research career under his guidance and for his constant enthusiasm and support over the past 3.5 years. My time in the lab has been truly transformative in my educational and personal development and I am forever grateful to Dr. Hursting for allowing me to discover a profound passion for scientific discovery. I would also like to thank Mike Coleman for three years of lessons, jokes, and some of the most outstanding mentoring a young researcher could ask for. His insights into how to think like a scientist are something that I will carry with me for the remainder of my career. I am truly grateful for Mike's patience, friendship, and commitment to advancing my scientific development and future opportunities.

TABLE OF CONTENTS

LIST OF FIGURES

LIST OF ABBREVIATIONS

AKT	Protein kinase B
CAF	Cancer associated fibroblast
ETC	Electron transport chain
FCCP	Carbonyl cyanide-4-(trifluoromethoxy)phenylhydrazone
FCR	Flux control ratio
FH	Fumarate hydratase
GDH	Glutamate dehydrogenase
GLS	Glutaminase
GSEA	Gene set enrichment analysis
HRR	High-resolution respirometry
ICI	Immune Checkpoint Inhibitor
INPP4B	Inositol polyphosphate 4-phosphatase type II
LDH	Lactate dehydrogenase
MCT	Monocarboxylate transporter
ME1	Malic enzyme-1
METABRIC	Molecular Taxonomy of Breast Cancer International Consortium
NK	Natural killer
OCR	Oxygen Consumption Rate
PC	Pyruvate carboxylase
PD1	Programmed cell death protein-1
PDH	Pyruvate dehydrogenase
PDK-1	Pyruvate dehydrogenase kinase-1

PDL-1	Programmed cell death protein ligand-1
PI3K	Phosphoinositide 3-kinase
PTEN	Phosphatase and tensin homolog
ROS	Reactive oxygen species
ROX	Residual oxygen consumption
SDH	Succinate dehydrogenase
SUIT	Substrate-uncoupler-inhibitor-titration
TAM	Tumor-associated macrophage
TCA	Tricarboxylic acid cycle
TIL	Tumor infiltrating lymphocyte
TME	Tumor microenvironment
TNBC	Triple-negative breast cancer
TNF-α	Tumor necrosis factor alpha
T_{reg}	T-regulatory cell
VISTA	V-domain immunoglobulin suppressor of T cell activation

CHAPTER 1: INTRODUCTION

Breast Cancer Prevalence and Progression

Breast cancer is a major public health concern worldwide and in the United States, making up 11.7% of the estimated 19.3 million new cancer cases across the globe in 2020[1]. In the US, breast cancer remains the most commonly diagnosed cancer amongst women, excluding basal and squamous cell skin cancers, with an estimated 281,000 new cases in 2021 alone[2]. Breast cancer also ranks as the second deadliest cancer amongst women in the US behind lung cancer, with the 5-year relative survival rate for all breast cancer stages combined currently at 90%[2]. While advances in treatment and early detection have yielded a 5-year relative survival rate upwards of 99% for localized breast cancer, metastatic breast cancer remains largely incurable with the 5-year relative survival rate dropping to approximately 25%[3].

Breast cancer is a heterogeneous disease with prognoses and treatment options that vary greatly between subtypes[4]. Amongst these subtypes, triple-negative breast cancers (TNBC), defined by negative expression of the estrogen receptor and progesterone receptor and lacking overexpression of the HER2 protein, have the most aggressive clinical manifestations and poorest prognoses[5]. The poor outcomes of TNBC patients are attributed to a lack of targeted therapies coupled with increased instance of metastasis and reoccurrence, with the 5-year relative survival rate for patients with metastatic TNBC dropping to 12%[6]. As TNBC is generally not sensitive to molecular or endocrine-based therapies[7], cytotoxic chemotherapy remains the standard of care. Therefore, investigation into metabolic dependencies of TNBC may aid in developing new therapeutic targets to augment current insufficient treatment options.

Metabolic Reprogramming in Breast Cancer

A fundamental requirement of rapidly dividing neoplastic cells is a rewiring of cellular metabolism to support the energetic and biosynthetic needs of cell growth. In the early 20th century, Otto Warburg made several seminal discoveries in how cancer cells reprogram their energy metabolism relative to the tissue of origin. Referred to as the Warburg effect, his findings described the propensity of cancer cells to markedly increase their glucose uptake and preferentially ferment pyruvate to lactate rather than utilizing mitochondrial oxidative phosphorylation, even in the presence of adequate oxygen[8, 9]. This metabolic phenotype of aerobic glycolysis is seen in a multitude of cells during rapid proliferation, from yeast to lymphocytes, suggesting a fundamental role in enhancing the rate of cellular division[10]. Although Warburg believed this metabolic phenotype (and the primary cause of cancer) to be due to defective mitochondria, substantial evidence since his discoveries have revealed cancer cells to possess largely functional mitochondria that still supply the majority of ATP for the cell[11, 12]. Investigation into what the proliferative advantage that aerobic glycolysis provides is still ongoing, as the fermentation of pyruvate to lactate is a highly inefficient means by which to produce ATP relative to complete glucose oxidation through the tricarboxylic acid (TCA) cycle. Numerous theories have been proposed including increased substrate availability for biomass production, faster ATP generation kinetics, and maintenance of cellular redox balance when demand for oxidative equivalents surpasses the need for ATP[13-15]. In order to fuel their extensive metabolic needs, cancer cells evolve oncogenic alterations that enhance glucose and amino acid uptake and often render them independent of growth-factor signaling[16]. Common genetic alterations such as those involved in the phosphoinositide 3-kinase (PI3K)/protein kinase B (Akt) signaling axis and its negative regulators phosphatase and tensin homolog (PTEN) and

inositol polyphosphate 4-phosphatase type II (INPP4B), as well as activating mutations in a variety of upstream receptor tyrosine kinases results in constitutive glucose utilization independent of environmental cues[17]. Though glycolytic flux is nearly ubiquitously enhanced in cancer, mitochondrial function and respiration are still required for tumor growth and play a vital role in cancer metabolism[18, 19]. In addition to bioenergetic functions, mitochondria provide substrates necessary for tumor anabolism, mediate redox balance, regulate apoptosis, and signal oncogenic programing through metabolites and reactive oxygen species (ROS)[20-23]. Mutations to enzymes involved in the TCA cycle including succinate dehydrogenase (SDH), fumarate hydratase (FH), and isocitrate dehydrogenase result in the production of metabolites which promote tumorigenesis[24-26]. Thus, reprogramming of both glucose and mitochondrial metabolism is required during the development and progression of cancers.

In addition to fueling the biosynthetic and energetic needs of aerobic glycolysis and other metabolic dependencies of proliferating cancer cells, the dysregulated uptake and efflux of nutrients has a profound effect on the tumor microenvironment (TME)[27]. The TME consists of a diverse array of malignant and nonmalignant cells that exist in a dynamic intercellular communication network mediated by metabolites, growth factors, cytokines, and various other signaling molecules[28]. Found within the TME are stromal cells, immune cells, endothelial cells and non-cellular components of extracellular matrix such as collagen and fibronectin[29]. Cancer-associated fibroblasts (CAFs) are the most numerous cell population in the tumor stroma, especially in breast cancers[30]. CAFs possess multiple pro-tumor functions in the TME, with direct effects on tumor growth, angiogenesis, invasion, and immunosuppression[31-33]. In addition, CAFs are key mediators of tumor metabolism by supplying energy rich metabolites such as lactate and pyruvate, fueling the TCA cycle for neighboring cancer cells[34]. In this

"reverse Warburg effect" model, cancer cells secrete hydrogen peroxide into the TME to induce oxidative stress and aerobic glycolysis in CAFs, resulting in the efflux of lactate that can be utilized as an anaplerotic carbon source for cancer cell mitochondrial metabolism[35, 36]. Similarly, multiple metabolic sub-populations of tumor cells exist within the TME in part due to varying access to the tumor vasculature and oxygen levels, with hypoxia resulting from incomplete vascularization being a common occurrence in solid tumors[37]. Cancer cells lacking adequate access to oxygen will preferentially uptake glucose to fuel glycolysis and efflux lactate, which cells in oxygenated zones of the tumor can uptake and utilize for oxidative phosphorylation[38]. Hence, a major barrier to successful implementation of metabolic-based therapeutics lies in overcoming the metabolic heterogeneity of the tumor.

In addition to the metabolic reprogramming that evolves throughout primary tumors, the ability of a tumor to metastasize to other organs is also dependent on metabolic adaptations to the unique stressors of migration to, and colonization of, a new tissue's microenvironment[39]. The process of metastasis involves multiple discrete steps including: invasion through the basement membrane, intravasation into and extravasation from the vasculature, and survival within the circulatory system and secondary tissue[40]. Though aggressive tumors are thought to release thousands of cells into the circulation each day, metastasis is a highly inefficient process with the large majority of these cells dying either in circulation or upon entry into distant organs[41, 42]. The metabolic reprogramming observed in metastatic cells is diverse, with the selection of metabolic programs conferring survival advantages throughout the metastatic cascade differing between tissues of origin and the secondary site[43]. Gene expression analysis of 20 different cancer types found downregulation of mitochondrial genes to be associated with the worst clinical outcomes and heightened expression of epithelial-to-mesenchymal transition

signatures[44]. Suppression of mitochondrial oxidative metabolism may promote tumor metastasis via limiting mitochondrial ROS generation, endowing cells in circulation a resistance to excess ROS-driven anoikis[45]. In breast cancer, metabolic flexibility is associated with enhanced metastatic potential, with aggressive breast cancer cell lines displaying increases in both glycolytic and oxidative metabolism[46]. The most common sites for metastatic spread from the breast are to the bone, lung, brain, and liver, with each possessing varying levels of oxygen and nutrient concentrations[47]. Hence, the potential for metastasis likely exists in a subset of primary tumor cells that have the metabolic flexibility to adapt to these unique environments who are then subjected to the additional selective pressures of metastatic spread[48]. Further, breast cancer cell lines with broad metastatic potential enhance both glycolysis and oxidative phosphorylation, while cell lines with site-selective metastatic potential primarily enhance either oxidative phosphorylation (lung or bone metastases) or glycolysis (liver metastases)[46]. Targeting of both metabolic dependencies has thus shown success in mouse models, with inhibition of either glycolysis or mitochondrial metabolism suppressing metastatic spread to varying degrees[49-51]. Thus, the study of metabolic reprogramming pertaining to breast cancer must consider the shared requirements of the primary tumor, the metastatic cascade, and the unique metabolic requirements of the various secondary organs.

The Role of Pyruvate Carboxylase in Breast Cancer Metabolism

Mitochondria are required for the production of numerous anabolic substrates necessary for cellular division, with many of the precursors used to synthesize nucleotides, amino acids, and lipids generated within the mitochondrial TCA cycle[52]. To maintain steady state levels of TCA cycle intermediates during constant efflux of biosynthetic substrates, mitochondria require an influx of carbon beyond the entry of the 2-carbon molecule acetyl-coA

following the pyruvate dehydrogenase (PDH) reaction. In a process termed anaplerosis, an influx of 4- or 5-carbon molecules allows for the refilling of oxaloacetate pools for subsequent condensation with acetyl-coA and continued flux through the TCA cycle[53]. The primary anaplerotic reactions that support cancer metabolism are the pyruvate carboxylase (PC)-mediated conversion of pyruvate to oxaloacetate and the serial conversion of glutamine to glutamate to α-ketoglutarate via the sequential reactions of glutaminase (GLS) and glutamate dehydrogenase (GDH)[54, 55]. PC-derived oxaloacetate serves multiple biosynthetic roles dependent on tissue and energy status, including: conversion to phosphoenolpyruvate via phosphoenolpyruvate carboxykinase in the gluconeogenesis pathway in the liver and kidneys, de novo fatty acid synthesis and glyceroneogenesis in adipocytes, and glucose-induced insulin secretion and glutathione synthesis in pancreatic islet cells[56]. Thus, PC has the potential to mediate metabolic reprogramming in cancer through the regulation of glucose metabolism, fatty acid synthesis, and protection from oxidative stress[57]. In most cancers, glutamine serves as the major anaplerotic carbon source, contributing to up to 90% of oxaloacetate pools[58]. However, PC is required for glucose-dependent anaplerosis and is the preferred anaplerotic enzyme in glutamine-independent cells that possess mutations to either SDH or FH, suggesting that both pathways are able to support mitochondrial metabolism in cancer[59-61].

PC expression is upregulated in multiple cancers relative to normal tissue, including lung, gallbladder, papillary thyroid cancer, and some breast cancer subtypes[57]. Analysis of the Molecular Taxonomy of Breast Cancer International Consortium (METABRIC) dataset found that 16-30% of breast cancer patients demonstrated copy number gains in PC[62]. Importantly, patients within the METABRIC data set that possessed PC gene amplification had significantly reduced survival times as compared to the rest of the cohort[62]. Immunohistochemistry staining

from tissue sections collected from 57 breast cancer patients similarly found PC to be highly expressed in cancerous samples relative to normal breast tissue[63]. In vitro, PC is upregulated in highly invasive breast cancer cell lines such as MDA-MB-231 relative to less invasive breast cancer lines[64]. Inhibition of PC in MDA-MB-231 cells via microRNA targeting or small molecule inhibitors results in diminished proliferation and cell migration in vitro and reduced tumor growth and metastasis in mouse models[65, 66]. In accordance with its role as one of the primary anaplerotic enzymes, suppression of PC in breast cancer cells results in lowered glucose incorporation into downstream metabolites of oxaloacetate, including malate, citrate, aspartate, and fatty acids[64]. The active metabolite of vitamin D, 1α,25-dihydroxyvitamin D ($1,25(OH)_2D$), transcriptionally downregulates PC and promotes oxidative stress and inhibition of de novo fatty acid synthesis[67, 68]. Further, exogenous oxaloacetate rescued MCF10A-ras cells from $1,25(OH)_2D$ induced sensitivity to oxidative stress[67]. The relationship between oxaloacetate availability and resistance to oxidative stress is likely through maintaining the substrate pool for the production of NADPH via malic enzyme (ME1), as NADPH is required for maintaining reduced glutathione for resistance to oxidative stressors[69, 70]. These in vitro studies suggest that PC-mediated glucose incorporation into oxaloacetate is required for the sufficient supply of substrates in pathways related to fatty acid synthesis and oxidative stress resistance in aggressive breast cancer cell lines. Both of these pathways are associated with metastatic progression and poor prognoses in human breast cancers[71, 72], which may in part explain the reduced survival of patients with PC gene amplification seen in the METABRIC analysis described by Shinde et al.[62].

In agreement with the role of PC in the proliferation and migratory potential of invasive breast cancer cell lines in vitro, PC is required for breast cancer metastasis to the lung in

mouse models. Tail vein injection of 4T1 murine mammary cancer cells with genetic PC depletion found PC suppression to have no effect on primary tumor size or non-pulmonary metastasis, but dramatically decreased pulmonary metastasis relative to PC-expressing cells[62]. In vivo ^{13}C glucose tracer analysis revealed breast cancer derived lung metastases to possess increased PC dependent anaplerosis relative to the primary tumor[73]. These data are well supported by the literature surrounding the role of PC in lung cancer, in which non-small cell lung tumors require pyruvate carboxylase for in vivo growth and are less dependent on glutamine relative to cell lines in culture[74]. The enhanced requirement for PC in the lung relative to other metastatic sites is likely a product of the lung microenvironment, characterized by higher oxygen content and increased oxidative stress which directs aerobic utilization of pyruvate[75]. In contrast, under hypoxic conditions of primary tumors and extrapulmonary metastases, HIF-1α directs glucose-derived carbons into lactate production rather than through the mitochondria via expression of hexokinase, lactate dehydrogenase (LDH), and pyruvate dehydrogenase kinase-1 (PDK1)[76]. Interestingly, in cases of clinical PC deficiency, a rare autosomal recessive disorder, patients commonly present with severe serum lactic acidosis due to the intracellular buildup of pyruvate and the subsequent conversion and export of lactate[77]. Thus, PC sits at the nexus of glycolytic and aerobic mitochondrial metabolism, with its downregulation likely supporting Warburg-like metabolism in hypoxic and glutamine-dependent cells and its upregulation supporting the growth of tumors in metabolic environments that require aerobic utilization of pyruvate such as the lung. A deeper understanding of the mechanisms by which PC differentially affects tumor growth at the primary and secondary site in various organs would help to refine the contexts in which targeting of PC may be beneficial in cancer therapy.

Cancer Metabolism's Role in Immune Evasion

Evasion of immune destruction is a hallmark of cancer and has burgeoned the growth of immunotherapies into the pillars of treatment for several forms of cancer[17]. Though some cancers show tremendous response to immunotherapies that have revolutionized their treatment, including hematologic and some solid tumors (e.g. melanoma), many cancers, including breast, have seen only modest benefits in a subset of patients[78]. One of the major barriers to treatment efficacy in solid tumors is immunosuppression of the TME through multiple mechanisms including immune cell exclusion, promotion of intrinsic immune cell inhibitory pathways, and/or an overabundance of regulatory immune cells[79]. The dysregulated metabolism of tumors can contribute to an immunosuppressed TME by regulating the availability of nutrients and presence of metabolic waste products that immune cells are exposed to upon infiltration[80]. The metabolic demands of activated immune cells are similar to proliferating tumors cells, with a marked increase in glucose and glutamine consumption mediated by HIF-1α and MYC signaling seen upon activation of T cells, natural killer (NK) cells, macrophages, and dendritic cells[81-83]. These parallel metabolic requirements may lead to competition within the TME for glucose, allowing tumors to metabolically restrict the activation of cytotoxic $CD8^+$ T cells and promote tumor progression[84]. In contrast, T regulatory (T_{reg}) cells rely primarily on fatty acid oxidation and oxidative phosphorylation to support their differentiation and function[85, 86]. Thus, glucose deprivation in the TME may alter the relative proportion of cytotoxic T cells to T_{reg} cells by starving the former while having minimal impact on the latter. A heightened ratio of T_{reg} cells to $CD8^+$ T cells negatively correlates with survival in breast cancer patients[87].

In addition to the competition for glucose, infiltrating immune populations must adapt to an acidic microenvironment with high levels of lactate mediated by glycolytic tumors and stromal cells[88]. Though lactate concentrations in the blood and healthy tissues typically range from 1.5-3.0mM, tumors can produce up to 20 times more lactate than normal tissues, resulting in TME lactate concentrations as high as 30mM[89, 90]. Lactate is an immunosuppressive metabolite to both innate and adaptive immune cells, driving anergy and reduced cytotoxic function in $CD8^+$ T-cells, inhibition of antigen presentation by dendritic cells, and polarization of tumor associated macrophages (TAMs) toward a "wound healing" M2-like phenotype[91-93]. These immunosuppressive effects are deleterious to immune surveillance in cancer, with LDHA suppression in melanoma cells leading to impaired growth of tumors in immune-competent C57BL/6 mice, yet having no effect in immunodeficient mice[94]. The export of lactate via the monocarboxylate transporter (MCT) family is accompanied by the export of H^+ ions, resulting in acidification of the TME which can independently drive immunosuppression[95]. Lowering in vitro conditions to pH levels similar to that found in the TME establishes an anergic state in human and mouse $CD8^+$ T cells[96]. The inhibitory immune checkpoint V-domain immunoglobulin suppressor of T cell activation (VISTA) mediates the suppression in T cell activity in response to reduced pH[97]. Though prolonged incubation in high lactate concentrations leads to cell death in up to 60% of $CD8^+$ T cells, similar incubations in an acidic environment without lactate had no such effect, suggesting TME acidification alone is insufficient to fully explain lactate-mediated immunosuppressive effects[98]. The combination of high lactate levels and reduced pH is correlated with limited efficacy of immunotherapies and poorer clinical outcomes[99]. Inhibition of lactate production and pH buffering restores cytotoxic T-cell function, reduces T_{reg} activation markers, and increases the efficacy of immunotherapy[94,

100]. Interestingly, PC may play a role in the development of drug resistance to lactate metabolism inhibitors such as AZD3965, an MCT1 specific inhibitor. Chronic exposure of human lymphoma and colon carcinoma to AZD3965 resulted in increased expression of PC and PDH, allowing for the re-oxidation of lactate to pyruvate and subsequent entry into the mitochondria to overcome energy deprivation caused by the suppression of glycolysis following MCT1 inhibition[101].

There are currently two immunotherapy agents that have been approved by the FDA for treatment of TNBC in combination with chemotherapy: pembrolizumab and atezolizumab. Both of these drugs belong to the class of immunotherapies termed immune checkpoint inhibitors (ICI) and specifically target the programmed cell death protein 1 (PD1) and its ligand (PDL1), respectively. PD1 is an inhibitory receptor expressed by all T cells during activation as well as B cells and some myeloid cell populations[102]. PD1 engagement by its ligands is critical for maintenance of peripheral tolerance but compromises anti-tumor immunity[103]. The cytoplasmic tail of PD1 contains two tyrosine-based structural motifs which recruit inhibitory phosphatases that downregulate both T cell receptor signaling and co-stimulatory CD28-mediated PI3K signaling[104]. Metabolic reprogramming is an important component of PD1-mediated suppression of T cell effector functions, with ligated PD-1 suppressing PI3K-AKT-mTOR signaling to impair glucose and glutamine utilization while promoting fatty acid oxidation via upregulation of AMPK[105, 106]. ICI's thus rescue the effector function of tumor-infiltrating lymphocytes (TILs) in part by acting as a metabolic therapy through restoration of glycolysis and anabolic mitochondrial pathways. As the nutrient milieu of the TME may also augment or abate such pathways, combination therapies involving metabolic inhibitors with ICI's may offer a novel approach to enhancing treatment efficacy. Importantly, the shared

metabolic requirements of tumor cells and activating TILs may complicate such approaches, highlighting the need for further study into the relationship of various metabolic pathways and anti-tumor immunity.

Project Goals

PC is now recognized as a crucial regulator of breast cancer metabolism and pulmonary metastatic potential. Modulation of PC expression likely results in downstream effects on the TME through its inverse relationship with lactate production, exemplified by the severe serum lactic acidosis seen in patients with PC deficiency. As lactate can serve as both a metabolic fuel and a potent immunosuppressive metabolite, this study investigated the potential role of PC in modulating the relationship between ICI and metabolic therapies targeting lactate. Though the effect of PC in pulmonary metastasis is well documented, the role of PC in the metabolic reprogramming of primary tumors has not been fully elucidated. Hence, the effect of in vitro PC suppression on central carbon metabolism and mitochondrial function was also assessed to delineate the role of PC in directing the metabolic reprogramming seen in primary mammary tumors.

This project adds to the growing body of literature surrounding the role of PC in breast cancer metabolism; testing the hypothesis that downregulation of PC in the primary tumor shunts a greater proportion of carbon through lactate dehydrogenase rather than into anabolic and energetic pathways that branch from the mitochondrial TCA cycle. In contrast to the oxygenated TME found in the lung, this metabolic phenotype is likely advantageous in primary mammary tumors and non-pulmonary secondary tumors in part by forming a pro-tumor microenvironment mediated by lactate. By identifying other pro-tumor mechanisms driven by PC suppression, this

project will also inform future investigations into targeted therapeutic approaches to enhance the efficacy of currently used chemo- or immunotherapies.

CHAPTER 2: METHODS

Cell Lines and Reagents

Wnt-1 oncogene-driven murine mammary cancer cells (M-Wnt) were used as the parental cell line for each knockdown. M-Wnt cells transduced with lentiviral particles containing a doxycycline-inducible short hairpin RNA (ShRNA) targeting PC construct (Smartvector) were a kind gift from Dr. D. Teegarden (Purdue University, Indiana). Vectors encoding shRNA constitutively targeting PC (ShPC-B, C, as well as a scramble construct, Sh-Scr) were purchased from Genecopoeia's shRNA construct product pipeline. These vectors were co-transfected into HEK293T cells along with a psPAX2 packaging construct and a PMD1.G viral envelope construct (both purchased from Addgene) to produce viral particles. After 24 hours, transfected HEK293T cell media was collected with a Luer-lock syringe, filtered through a 0.45-micron syringe filter, and added directly to M-Wnt cells. Addition of lentivirus-containing media from transfected HEK293T cells onto M-Wnt cells was repeated once more at 48 hours post-transfection. After 48 hours of viral infection, successfully infected M-Wnt cells were selected for with 1mg/mL hygromycin for at least 96 hours or until all untransduced control cells died. PC knockdown was confirmed with RT-qPCR.

Reverse siRNA transfection of M-Wnt cells using 10nM ON-TARGETplus SMARTpool PCx siRNA (Drahmacon, Lafayette, CO) was used as an orthogonal approach to suppress PC expression (Si-PC). 10nM Ambion silencer negative control siRNA cat#4390843 (ThermoFisher Scientific, Waltham, MA) was used as a negative control (Si-Scr). Lipofectamine3000-RNAiMAX reagent (Invitrogen, Carlsbad, CA) was used for the

siRNA transfection. Each siRNA and the lipofectamine were diluted separately in Gibco Opti-MEM and then mixed and incubated at room temperature for 15 minutes. The siRNA-lipofectamine mixtures were then added to a resuspension of M-Wnt cells in HPLM at a concentration of 150,000 cells/mL and seeded for RT-qPCR and flow cytometry the following day.

Cell lines were maintained at 37°C and 5% CO_2 in Gibco RPMI 1640 Medium supplemented with 10% fetal bovine serum (FBS), 2mM glutamine, and 50IU/mL penicillin/streptomycin. For all in vitro assays, cells were seeded and collected in Gibco Human Plasma-Like Medium supplemented with 10% FBS and 50IU/mL penicillin/streptomycin to resemble the natural metabolite concentrations of in vivo biological systems.

Animal Studies

All mouse studies were approved by the Institutional Animal Care and Use Committee of the University of North Carolina at Chapel Hill. Mice were housed in a climate-controlled Division of Comparative Medicine facility with ad libitum access to water and diet. Once tumors were palpable, tumor size was measured thrice weekly with digital calipers and tumor volume was calculated by length x width^2/2. All mice were euthanized by CO_2 inhalation followed by cervical dislocation.

For the pilot study utilizing doxycycline-inducible ShPC M-Wnt cells, 10 female C57BL/6 mice (Charles River Labs, Wilmington, MA) were injected in the 4th mammary fat pad with 50,000 doxycycline-inducible ShPC M-Wnt cells. Mice were randomized to the control or treatment group (n=5) with the treatment group having ad libitum access to water supplemented with 150μg/mL of doxycycline. Doxycycline supplementation began once tumors were palpable.

4 weeks following injection, mice were euthanized and tumors were excised, measured, weighed, and flash frozen.

In subsequent mouse studies, 50,000 of the constitutive ShPC knockdown cell lines were injected into the 4th mammary fat pad of female C57BL/6 mice (Charles River Labs, Wilmington, MA). In the study utilizing the ShPC-B and Sh-Scr cell lines, mice were randomized to receive either Sh-Scr or ShPC-B cell line injection and then further randomized into 4 treatment groups per condition (n=15). Scramble and ShPC-B injected mice were randomized to control or treated with FX11 (2mg/kg), anti-PD1 antibody (200μg/mouse), or a combination of FX11 and anti-PD1 antibody. Once tumors were palpable, mice underwent daily injections intraperitoneally with FX11 or its control (10% DMSO, 40% PEG300, 5% Tween, and 45% saline) and every three days with anti-PD1 antibody or its control (isotype control at 200 μg/mouse). 4 weeks following injection, mice were euthanized and tumors were excised, measured, weighed, and flash frozen ex vivo.

Gene Set Enrichment Analysis

The Omega E.Z.NA Total RNA Isolation Kit (BioTek, Winooski, VT) was utilized for extraction of total RNA from excised tumors following homogenization in TRIzol reagent. The isolated RNA was labeled and hybridized to a Clariom S HT array (ThermoFisher) and then processed by the UNC Functional Genomics Core. Gene expression data was analyzed with TAC 4.0 software correcting for batch effects (Affymetrix, Santa Clara, CA). Gene Set Enrichment Analysis (GSEA) utilizing the Hallmarks gene set was utilized for pathway enrichment analysis[107]. Mouse Gene Symbol Remapping to Human Orthologs (Version 7.2) was selected from the GSEA-MSIGDB file servers and ran with the default criteria and 1,000 permutations[108].

Lactate-Glo Assay

The Lactate-Glo Assay Kit (Promega, Wisconsin, USA) was utilized to detect intracellular and extracellular lactate concentrations in vitro. Control and PC knockdown M-Wnt cells were seeded in 6cm plates at a concentration of 400,000 cells per plate in HPLM. Following 24 hour incubation, HPLM was replaced with fresh media plus the respective experimental conditions (treatment group receiving 25μM FX11 and control group receiving 0.05% DMSO) for an additional 24 hours. Culture media for determination of extracellular lactate concentrations was deproteinated with 3KD spin filters for 20 mins at 16,000 RCF and then diluted 1:75 in PBS. Deproteinated media was then snap frozen in liquid nitrogen and stored at -80°C. For determination of intracellular lactate, cells were lysed in 200uL of 600mM HCl, neutralized with 200μL 1M tris base, diluted 1:1 in PBS, and frozen at -80°C. Remaining assay protocol was performed per supplier's instructions. Luminescence values were measured on a Cytation 3 Cell Imaging Reader (BioTek, Winooski, VT). Lactate concentrations were normalized to 1,000,000 cells per condition with cell counting via trypan blue exclusion.

MTT Cell Viability Assay

Control and PC knockdown M-Wnt cells were seeded at 2,500 cells per well in a 96 well plate in HPLM for 24 hours. Following incubation, cells were treated for an additional 24 hours with new HPLM supplemented with the respective experimental conditions (treatment group receiving FX11 at doses ranging from 6.25μM to 100μM and the control group receiving concordant concentrations of DMSO). Media was then aspirated and cells were washed with PBS and stained with 100μL of MTT solution (0.5mg/mL 3-(4,5-dimethylthiazol-2-yl)-2,5-diphenyl tetrazolium bromide in cell culture media without FBS). Cells were covered and incubated in MTT solution for 90 minutes. MTT reagent was then replaced with 100μL of

DMSO and plates were shaken for 15 minutes. Absorbance was measured using a Cytation 3 Cell Imaging Reader (BioTek, Winooski, VT) at 595 and 690nm. Absorbance values at 690nm were subtracted from absorbance values at 595nm. Cytotoxicity was calculated relative to untreated control.

mRNA Analyses

In vitro gene expression analysis was conducted on ShPC M-Wnt cells to confirm PC knockdown and determine further transcriptional changes. RNA was isolated from in vitro ShPC M-Wnt cells using the Omega E.Z.N.A HP Total RNA Isolation Kit (BioTek, Winooski, VT) according to manufacturer's instructions. cDNA was then synthesized using the ABI High-Capacity cDNA Reverse Transcription Kit (Thermo Fisher, Waltham, MA) and incubation in a thermocycler. cDNA was combined with Universal SYBR Green super-mix (BioRad, Hercules, CA). Mouse primer sequences were obtained from PrimerBank[109] and purchased from IDT (IDT, Coralville, IA). RT-qPCR was used to determine relative expression as calculated by $2^{-\Delta\Delta ct}$ as previously described[110].

Flow Cytometry

All flow cytometry was performed using a CytoFlex cytometer (Beckman Coulter, Brea, CA). ShPC M-Wnt cells were seeded at a concentration of 300,000 cells per well in a 6-well plate overnight in HPLM. Cells were harvested using PHEM buffer and stained for 30 minutes in MitoTracker Red dye (Invitrogen M7512) diluted 1:2,000 in PBS + 2mM EDTA and 2% bovine serum albumin (BSA). Following 30 minutes of staining, cells were strained through a FACS filtered tube and data was acquired on the CytoFlex cytometer. 15,000 single cell live events were collected for each sample. Cells stained in PBS buffer without addition of MitoTracker Red were used as controls to confirm staining.

Media Exchange Assays

To investigate the potential effects of PC-knockdown-mediated changes to media composition, Sh-Scr cells were seeded in collected culture media of the ShPC cell lines as well as fresh HPLM. Sh-Scr, B, and C cells were seeded at 1,000,000 cells per plate in a 10cm plate and incubated for 48 hours in HPLM. Sh-Scr cells maintained in RPMI were then resuspended and seeded in the 48 hour culture media of the various cell lines.

Extracellular Flux Analysis

Cellular Oxygen Consumption Rate (OCR) was determined using a XF96 Seahorse Metabolic Flux Analyzer (Agilent Seahorse Technologies, Santa Clara, CA). ShPC M-Wnt cells were seeded into a XF96 Seahorse cell cultures plate at a density of 5,000 cells per well in HPLM for 24 hours. Following incubation, HPLM was replaced with the respective experimental conditions (treatment group receiving 25μM duroquinone and control group receiving concordant concentration of ethanol) for an additional 24 hours. 1 hour prior to analysis, cells were incubated in assay media (serum-free RPMI-1640 media with 10mM glucose, 2mM glutamine, and 1mM pyruvate, without bicarbonate, pH 7.4) in a Non-CO_2 incubator. Oligomycin (1.0μM), carbonyl cyanide-4-(trifluoromethoxy)phenylhydrazone (FCCP; 1.0μM), and rotenone/antimycin A (0.5μM) were added sequentially as OCR was measured. OCR data was normalized by total protein amount using a bicinchonic acid protein assay (Thermo Fisher, Waltham, MA).

High-Resolution Respirometry

An established substrate-uncoupler-inhibitor-titration (SUIT) protocol for high-resolution respirometry (HRR) was utilized with in vitro M-Wnt cells (SUIT-001 O2 ce-pce DOO4, https://www.bioblast.at/index.php/SUIT-001_O2_ce-pce_D004). Cells were trypsinized,

counted, and re-suspended in Mir05 buffer (Oroboros Instruments, Innsbruck, Austria). 1,000,000 cells were injected into 2mL pre-calibrated Oxygraph-2k chambers (O2k, Oroboros Instruments, Innsbruck, Austria). Experiments were performed at 37°C under constant stirring with oxygen concentrations maintained between 100 and 200μM. Reoxygenation was performed via addition of 5μL of catalase (112,000U/mL dissolved in Mir05, Sigma C9322) and titration of hydrogen peroxide (50 wt. % in H_2O, Sigma 516813) until desired oxygen concentration was reached. Residual oxygen consumption (ROX) was measured after permeabilization with digitonin and subtracted from oxygen flux as a baseline for all respiratory states to obtain mitochondrial respiration. Specific flux was expressed as oxygen consumption per million cells (ρmol·s^{-1}·million cells). For determination of flux control ratios (FCR), respiration values were normalized to the internal reference state NS_E, achieved following addition of N- and S-coupled substrates and titration of carbonyl cyanide p-(tri-fluromethoxy)phenyl-hydrazone (FCCP) until complete uncoupling of the mitochondrial membrane potential was achieved. DatLab Software (V7.4, Oroboros Instruments) was utilized for data acquisition and post-experimental analysis.

Statistical Analysis

Data was analyzed using GraphPad Prism 9 software (GraphPad Software inc., San Diego, CA). Statistical analysis was determined using Student's t-test for comparisons of two groups and one-way analysis of variance (ANOVA) for comparisons of three or more groups. A three-way ANOVA was used for mouse studies comparing response of FX11, anti-PD1, or the combination of the two in Sh-Scr versus ShPC-B tumors. P-values less than 0.05 were considered significant. Significance of Hallmark gene sets was determined by a false discovery rate (FDRq) value of less than 0.05. Error bars are presented as mean ± standard error of mean (SEM).

CHAPTER 3: RESULTS

Pyruvate carboxylase suppression results in enhanced primary tumor growth

Though PC is required for pulmonary metastasis from mammary tumors in mouse models, the role of PC in the metabolism and growth of primary tumors is not fully understood. To investigate the effects of PC knockdown at the primary site, we first utilized a primary tumor model of TNBC with a doxycycline-inducible ShRNA construct targeting PC transduced into M-Wnt cells (ShPC). C57BL/6 mice were injected in the fourth mammary fat pad and randomized to treatment with or without doxycycline once tumors were palpable.

In contrast to previously described literature, PC knockdown of 60% expression relative to the control group resulted in increased primary tumor mass (**Fig. 1A-B**). Other groups have shown suppression of PC via small-molecule inhibition or genetic targeting to either diminish[65] or have no growth effect[62] on primary tumors in vivo, respectively. To investigate potential mechanisms underlying this novel pro-growth phenotype, transcriptomic analysis via isolated RNA from excised tumors was conducted to determine gene expression changes caused by PC suppression. Gene Set Enrichment Analysis (GSEA) was used to identify broad biological processes that were most affected by loss of PC. By ranking tumor-derived gene expression values within predefined gene lists by their relative expression between PC knockdown and control transcriptomes, GSEA allows for identification of pathways that were upregulated in one condition over the other. The Hallmarks gene sets contained 50 well-defined biological pathways with limited redundancy[107]. Of the 50 gene sets, 8 represent immunological pathways that encompass broad innate and adaptive immune processes. All 8 of

these pathways were found to be downregulated in the PC knockdown tumors relative to control, in addition to 2 gene sets involved with fatty acid metabolism (**Fig. 1C**). Based on the potential of this immunosuppressive signature to drive the pro-growth effect of PC knockdown, we next set out to determine potential metabolic mediators of the observed immunosuppression.

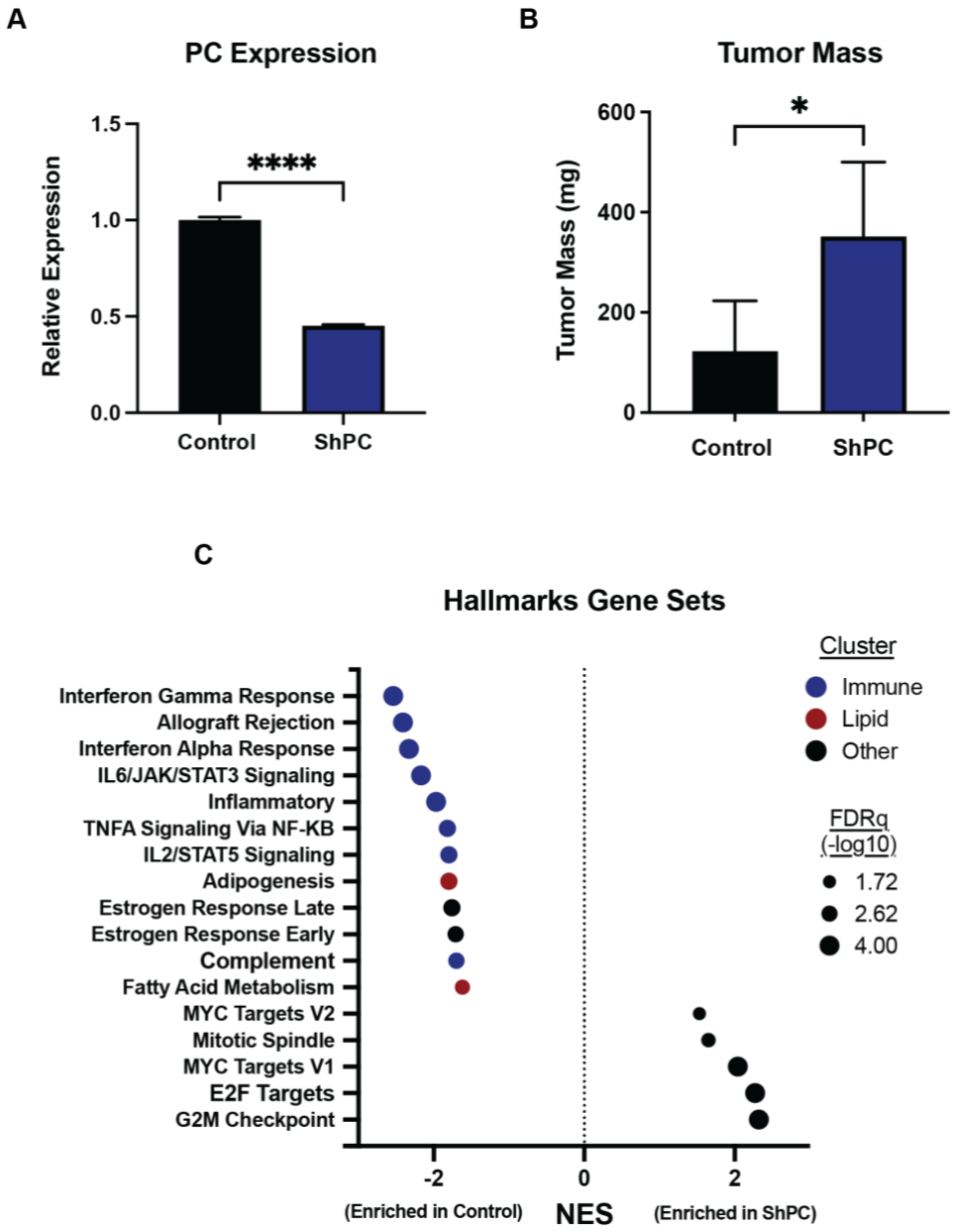

Figure 1: PC knockdown results in increased tumor mass and an immunosuppressed gene expression signature. Relative PC expression from isolated RNA of excised tumors (n = 5 per group) was assessed between mice treated with or without doxycycline (A). Ex vivo tumor mass at study termination (B). Significant normalized enrichment scores (NES) from the Hallmarks gene sets at FDRq of $p < 0.05$ (C). FDRq denoted by bubble size. All data presented with error bars representing means ± standard error of means (SEM). *p-values of < 0.05. ****p-values < 0.0001.

PC suppression enhances sensitivity of M-Wnt cells to inhibition of lactate metabolism

To investigate the mechanism and potential targets of PC knockdown-induced immunosuppression, we generated multiple constitutive PC knockdown M-Wnt cell lines via ShRNA targeting PC constructs (ShPC-B and ShPC-C), as well as a non-targeting shRNA control (Sh-Scr). We first utilized the ShPC-B cell line as it reproducibly generated the strongest PC knockdown of ~95% relative to control (**Fig. 2A**). As inherited PC deficiency commonly results in serum lactic acidosis and lactate is a potent immunosuppressive metabolite in the TME, we hypothesized lactate to be a key mediator of the immunosuppressive effect seen in the gene expression analysis. Hence, we assessed the effect of PC knockdown on lactate production in M-Wnt cells and if suppression of PC promotes sensitivity to inhibition of lactate metabolism. Knockdown of PC resulted in increased intracellular lactate concentrations relative to control (**Fig. 2B**). Treatment of control and ShPC-B cells with FX11, an LDHA specific inhibitor, significantly reduced intracellular lactate concentrations in the ShPC-B cells but had minimal effect on control cells (**Fig. 2B**). Further, ShPC-B cells showed increased cytotoxic sensitivity to FX11 across a range of doses, with treatment of 25μM FX11 showing the largest difference between PC knockdown and control (**Fig 2C**).

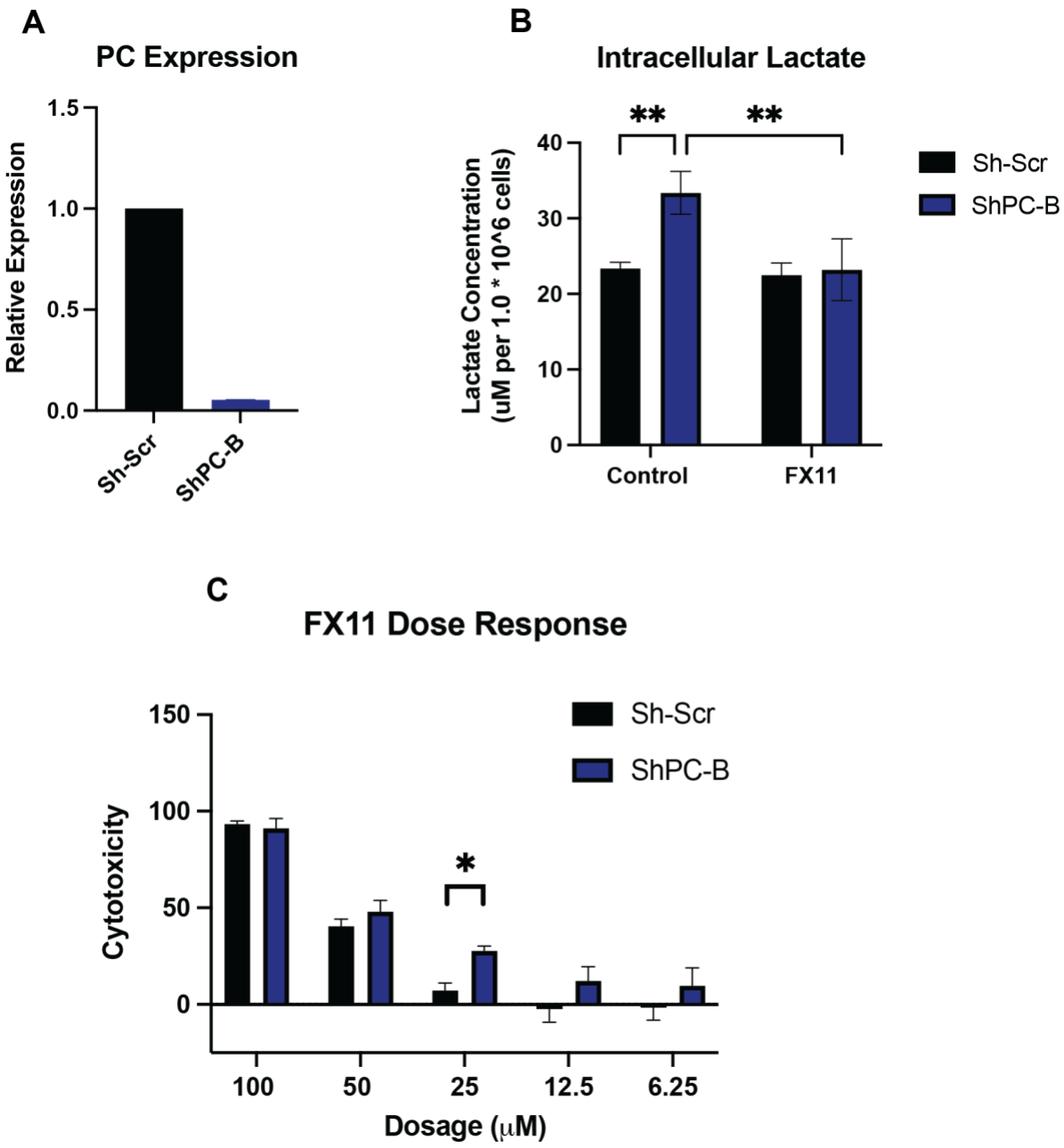

Figure 2: PC knockdown sensitizes M-Wnt cells to lactate dehydrogenase inhibition. Relative PC expression of the ShPC-B cell line relative to Sh-Scr (A). Intracellular lactate concentrations (μM) in Sh-Scr and ShPC-B cells with and without treatment of 25uM FX11 per million cells (B). Cytotoxicity of FX11 at doses ranging from 6.25-100μM (C). All data presented are the mean of 3 biological replicates with error bars representing means ± SEM. *p-value < 0.05, **p-values < 0.01.

PC knockdown of 95% expression is deleterious to mammary tumor growth

Given these findings that FX11 inhibits lactate production and is more cytotoxic in the ShPC-B cell line relative to control, we next tested the hypothesis that FX11 can be used to rescue the immunosuppressed TME observed in a mouse model and potentiate a response to ICI. C57BL/6 mice were orthotopically injected into the fourth mammary fat pad with either Sh-Scr or ShPC-B cell lines and randomized to receive either control injections, FX11 (2mg/kg), anti-PD1 antibody (200μg/mouse), or a combination of the two. We assessed the potential for toxicity of the FX11, anti-PD1 antibody, or combination treatment via bodyweight measurements and did not observe any differences amongst groups (**Fig. 3B**). PC knockdown of 95% expression resulted in reduced tumor mass relative to control in all treatment conditions (**Fig. 3A**), a direct contrast to the enhanced pro-growth effect seen in the doxycycline-inducible ShPC model that achieved a PC knockdown of 60% expression. All three treatment conditions did not alter the deleterious effect of PC knockdown, with no significant differences between the control and treatments in both the Sh-Scr and ShPC-B tumors (**Fig. 3A**).

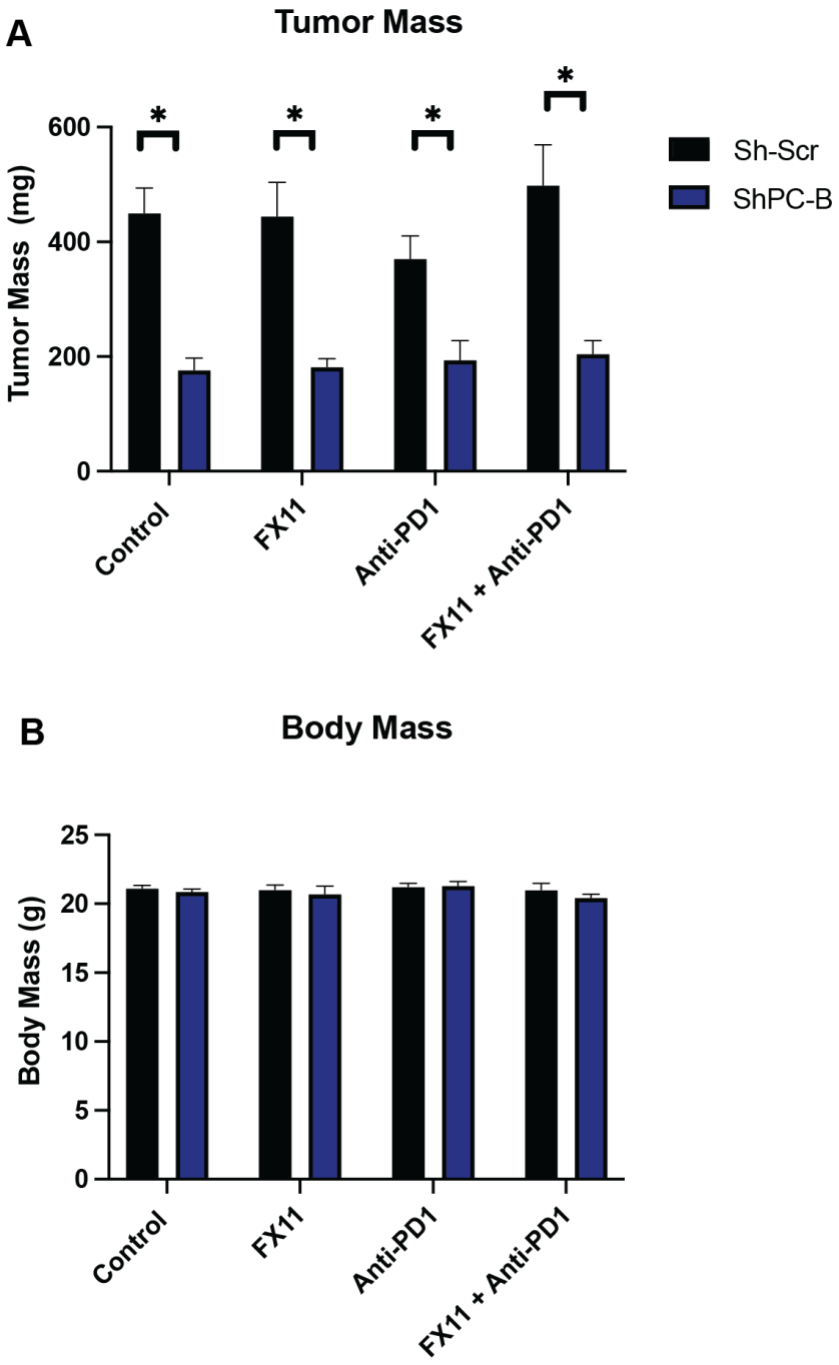

Figure 3: PC knockdown of 95% expression is deleterious to mammary tumor growth irrespective of metabolic and/or ICI therapies. Tumor mass weighed ex vivo following treatment of control injections, FX11, Anti-PD1 antibody, or a combination of the two treatments (A). Body mass of mice (n = 15 per group) at study termination (B). A three-way ANOVA was utilized to determine significant differences between groups, with no significant differences observed in body mass and only the effect of PC knockdown resulting in significant differences in tumor mass in all conditions. All data presented with error bars representing means ± standard error of means (SEM). *p-values of < 0.05.

To further investigate the contrast between the reduced tumor growth seen in the ShPC-B cells and the enhanced tumor growth seen in the doxycycline-inducible ShPC cells, we next utilized the ShPC-C cell line. The ShPC-C cells had a consistent PC knockdown of ~80% expression relative to the Sh-Scr line (**Fig. 4A**). The two knockdowns resulted in distinct effects on tumor growth relative to control, with the ShPC-B cells again resulting in significantly reduced tumor growth while the ShPC-C cells recapitulated the pro-growth effect we first identified in the doxycycline-inducible model (**Fig. 4B**).

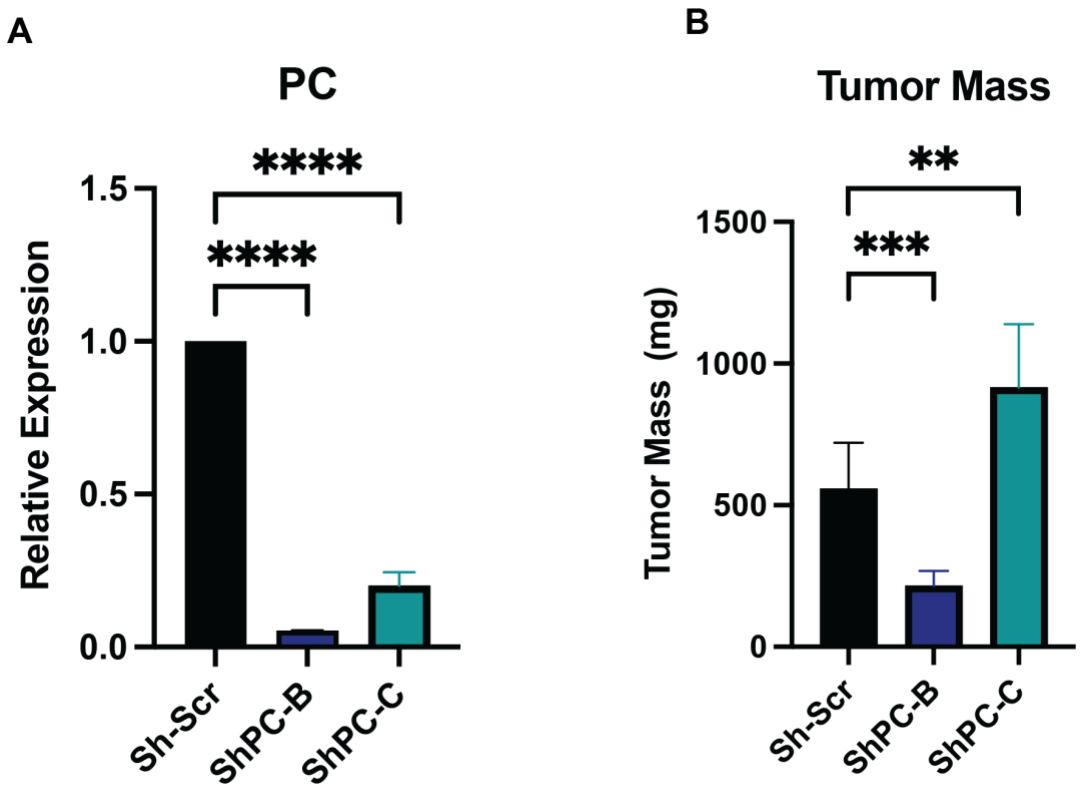

Figure 4: Distinct effects on tumor growth from two PC knockdown cell lines. In vitro relative PC expression of the ShPC-B and ShPC-C cell lines relative to Sh-Scr (A). Tumor mass weighed ex vivo at study termination (n=6 per group) (B). All data presented with error bars representing means ± standard error of means (SEM). **p-values < 0.01. ***p-values < 0.001, ****p-values < 0.0001.

Mitochondrial oxygen flux is variably altered by degree of PC suppression

Following these finding that the different knockdowns of PC can result in either a protumor or antitumor effect, we next set out to identify potential determinants of the dichotomous role of PC at the primary site. As PC catalyzes one of the primary anaplerotic reactions that maintains TCA cycle flux, we investigated potential functional and transcriptional mitochondrial differences between the PC knockdown cell lines. We hypothesized that PC suppression would alter mitochondrial metabolism and specifically the capacity of the cell to fuel oxidative phosphorylation. Utilizing extracellular flux analysis, we found both PC knockdown cell lines to have a reduced basal oxygen consumption rate (OCR) relative to control (**Fig. 5A**), with the ShPC-B knockdown resulting in a 13% reduction in OCR and the ShPC-C knockdown resulting in a larger 25% reduction. Following injection of the protonophore FCCP to achieve maximal ETC flux, i.e. flux that is no longer limited by complex V-mediated reductions to the protonmotive gradient, the OCR of both knockdowns was again reduced relative to control (**Fig. 5B**). This decrease in maximal oxygen consumption indicates that the reductions in basal OCR following PC suppression are not driven by complex V's capacity to reduce the protonmotive gradient during oxidative phosphorylation.

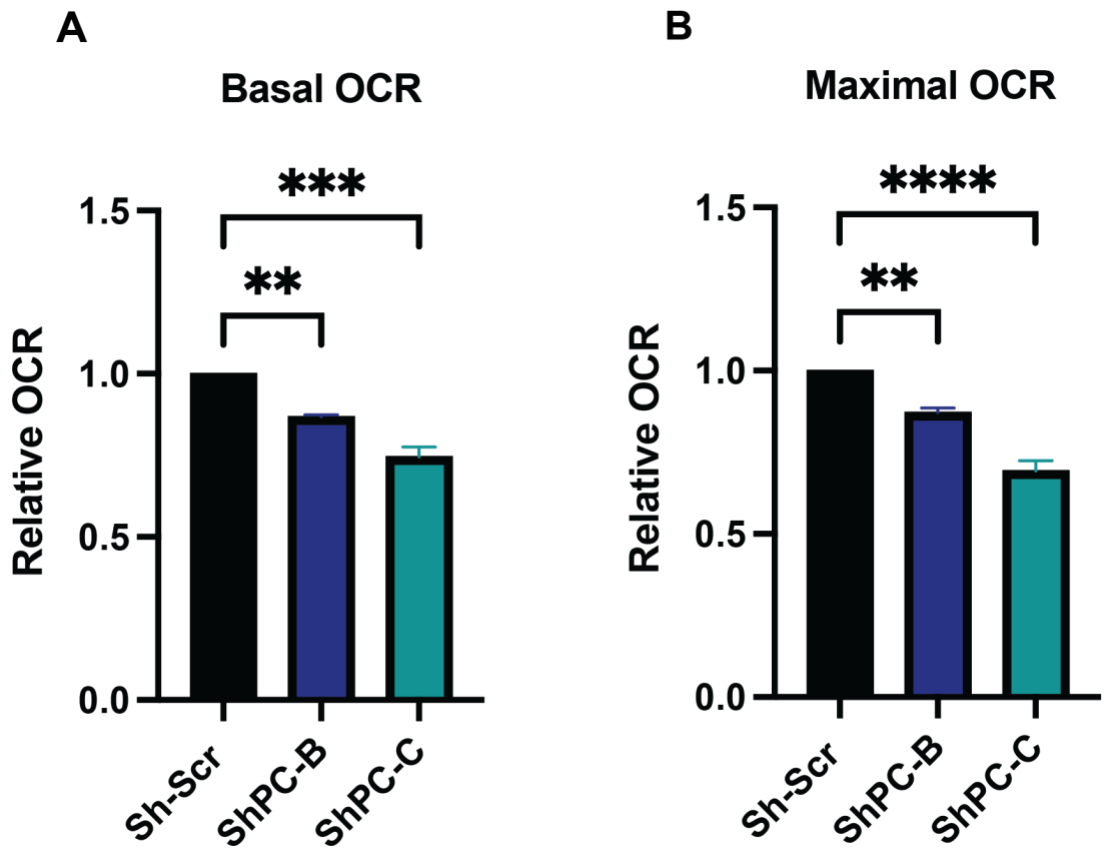

Figure 5: PC suppression reduces cellular respiration to varying degrees. Basal oxygen consumption rate of ShPC cells relative to Sh-Scr (A). Maximal oxygen consumption rate following injection of the protonophore FCCP to collapse the mitochondrial membrane potential (B). Data presented with error bars representing means ± standard error of means (SEM). **p-values < 0.01. ***p-values < 0.001.

Though extracellular flux analysis of intact cells lends valuable insight into cellular energetics, the ability of extracellular flux analysis to assay changes to mitochondrial ETC dynamics is limited. Hence, we next used high-resolution respirometry (HRR) to understand the effects of PC knockdown on ETC intrinsic function at the complex level. Oxygen flux was analyzed in permeabilized cells following sequential titrations of the NADH-linked (N-linked) substrates pyruvate, malate, and glutamate, the succinate dehydrogenase-linked (S-linked) substrate succinate, inhibitors of ETC complexes I (rotenone) and III (antimycin A), and the protonophore FCCP to assess respiratory coupling control of various electron transfer pathways

(**Fig. 6A**). In contrast to the reduction of basal and maximal OCR seen in extracellular flux analysis, the PC knockdown cell lines did not exhibit reduced oxygen flux across all pathway control states, with ShPC-B, in fact, showing increased levels of oxygen flux relative to Sh-Scr (**Fig. 6B**). The flux control ratios (control state specific OCR normalized to the maximum flux state achieved following addition of N- and S-linked substrates and titration of FCCP) were unchanged in both PC knockdown cell lines, indicating that PC suppression does not result in changes to intrinsic ETC flux control (**Fig. 6C**). These findings suggest that PC knockdown does not reduce basal oxygen consumption through driving intrinsic mitochondrial dysfunction or reprogramming of coupling controls, but likely results in reduced flux of intermediates through the TCA cycle to fuel the ETC and hence oxidative phosphorylation. In addition, ShPC-B cells appear to respond to PC knockdown by increasing efficiency of its ETC system.

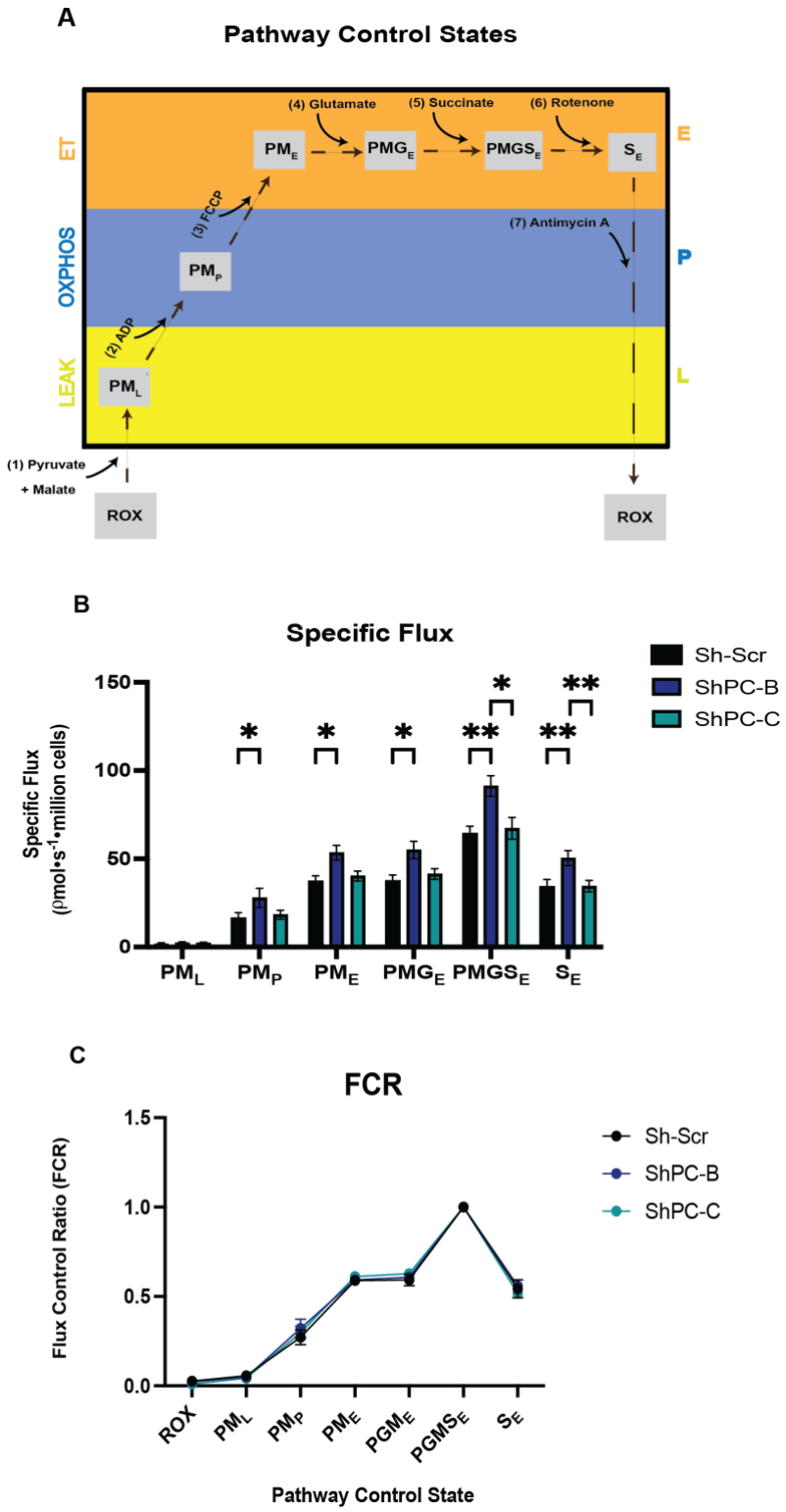

Figure 6: PC suppression does not reduce mitochondrial oxygen flux dynamics when mitochondria are rendered independent of cytosolic metabolism. Graphical description of the sequential steps of the substrate-uncoupler-inhibitor titration (SUIT) protocol utilized in high-resolution respirometry (A). Leak respiration (L) achieved following plasma membrane

permeabilization and pyruvate (P) and malate (M) titrations. Oxidative Phosphorylation (OXPHOS, P) achieved with saturating concentrations of adenosine diphosphate (ADP). Electron transport capacity (ET) following complete chemical uncoupling of the inner mitochondrial membrane with FCCP. Specific oxygen flux of the ShPC cells relative to Sh-Scr (ρmol·s^{-1}·million cells) (B). Flux control ratio (FCR) normalized to the internal reference state NS_E, achieved following addition of N- and S-coupled substrates and titration of FCCP until complete uncoupling of the mitochondrial membrane potential was achieved (C). Data presented are the means of 8 biological replicates with error bars representing means ± standard error of means (SEM). *p-values < 0.05. **p-values < 0.01.

PC knockdown results in varying degrees of ETC transcriptional changes

To further investigate the potential for PC suppression to induce changes to mitochondrial metabolism, we next set out to determine in vitro gene expression differences between the two knockdown cell lines. Relative gene expression of subunits of the electron transport chain (ETC) was determined to identify potential changes to the oxidative phosphorylation machinery in the face of PC suppression. PC knockdown of ~95% expression in the ShPC-B cell line resulted in downregulation of subunits that comprise complex I (*Nd4fa*10 and *Nd4fa10*), II (*Sdhb*), and V (*Atp5c1*), while ShPC-C only resulted in downregulation of *Atp5c1*, though to a lesser degree than ShPC-B (**Fig. 7A-F**). We next utilized flow cytometry to quantify the mitochondrial mass in the PC knockdown and scramble cells. ShPC-C had increased mitochondrial mass while ShPC-B had no significant difference relative to control (**Fig. 7G**).

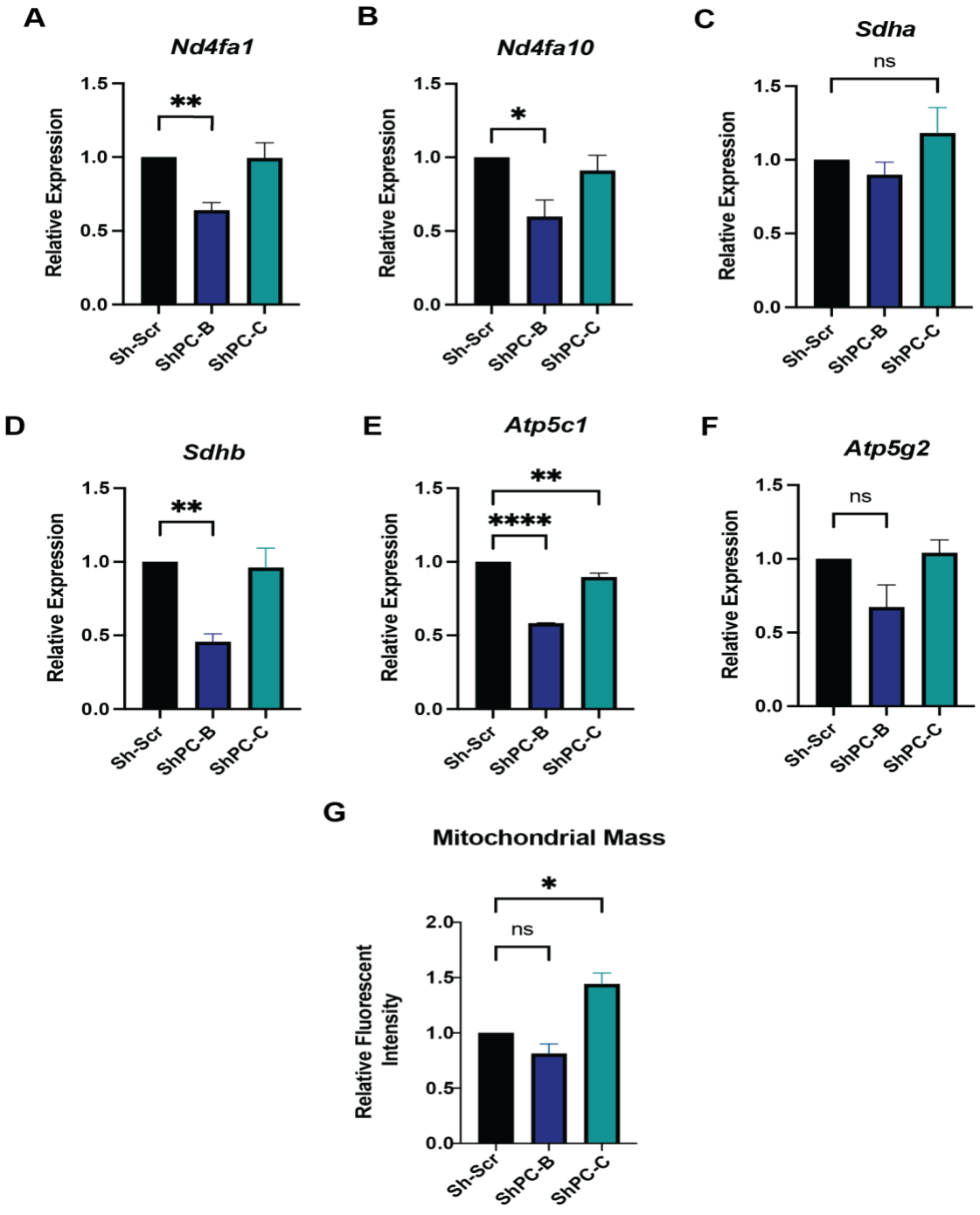

Figure 7: PC knockdown cell lines possess varying degrees of mitochondrial gene expression and mass changes relative to control. Relative gene expression of complex I, II, and V subunits in the ShPC-B and ShPC-C cell lines relative to Sh-Scr (n = 5 per group) (A-D). Relative fluorescent intensity of Sh-Scr versus ShPC-B and ShPC-C following staining with MitoTracker Red diluted 1:2,000 in PBS (n = 5 per group) (E). One-way ANOVA used to determine statistical significance ($p < 0.05$). All data presented with error bars representing means ± standard error of means (SEM). *p-values < 0.05.

The decrease in relative expression of multiple subunits of the ETC in response to PC knockdown in the ShPC-B cell line appeared in contrast to the findings of enhanced ETC efficiency seen in the HRR analysis. To investigate the hypothesis that the degree of PC knockdown drives varying degrees of alterations to ETC gene expression rather than these findings being an experimental artefact of the construct, we utilized on orthogonal approach to suppress PC expression via siRNA targeting. The Si-PC cells exhibited a knockdown similar to that of the ShPC-B cells, with approximately 92% reduced PC expression relative to control (**Fig. 8A**). The ETC gene expression changes of the Si-PC cells were similar to those seen in the ShPC-B cells, with decreased expression of subunits of complex I, II, and V relative to control (**Fig. 8B-G**). Mitochondrial mass was not statistically different in both the ShPC-B and Si-PC cells relative to their respective controls (**Fig. 8H**).

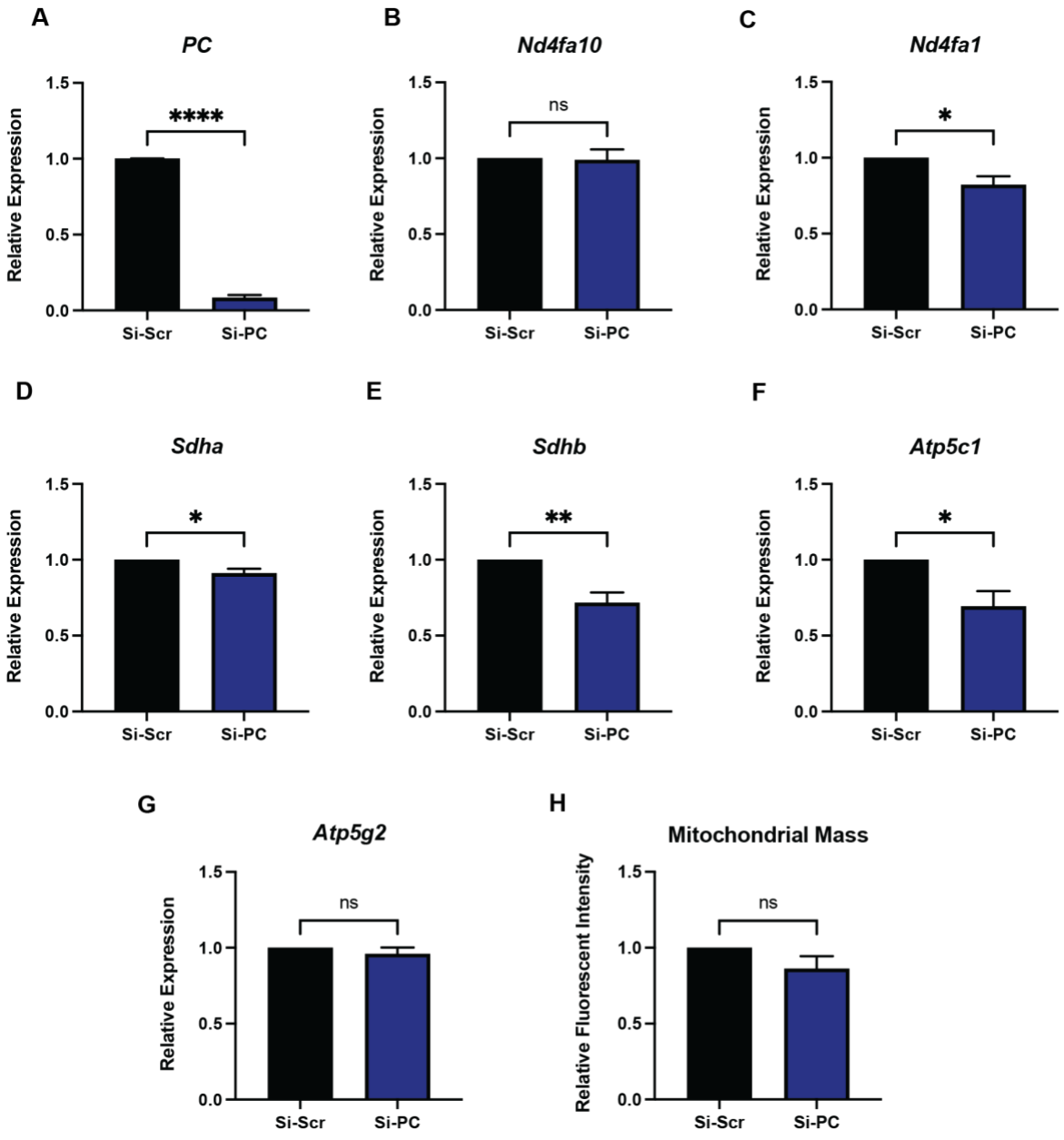

Figure 8: PC knockdown via small interfering RNA recapitulates mitochondrial gene expression and mass changes of short hairpin RNA construct. Relative gene expression of complex I, II, and V subunits in Si-PC M-Wnt cells relative to Si-Scr M-Wnt cells (n = 6 per group) (A-E). Relative fluorescent intensity of Si-Scr versus Si-PC M-Wnt cells following staining with MitoTracker Red diluted 1:2,000 in PBS (n = 6 per group) (F). All data presented with error bars representing means ± standard error of means (SEM). *p-values < 0.05. **p-values < 0.01. ****p-values < 0.0001.

To test whether the observed effects of in vitro PC knockdown were driven by intrinsic adaptation to loss of PC or through indirect mechanisms that result from changes to substrate efflux, we seeded the Sh-Scr cells in the cell culture media from the PC knockdown cell lines and again measured changes in ETC gene expression and mitochondrial mass. Sh-Scr cells were seeded in 48 hour culture media from Sh-Scr, ShPC-B, or ShPC-C before being collected for RT-qPCR and flow cytometry. None of the conditions resulted in changes to ETC gene expression or mitochondrial mass (**Fig. 9A-E**).

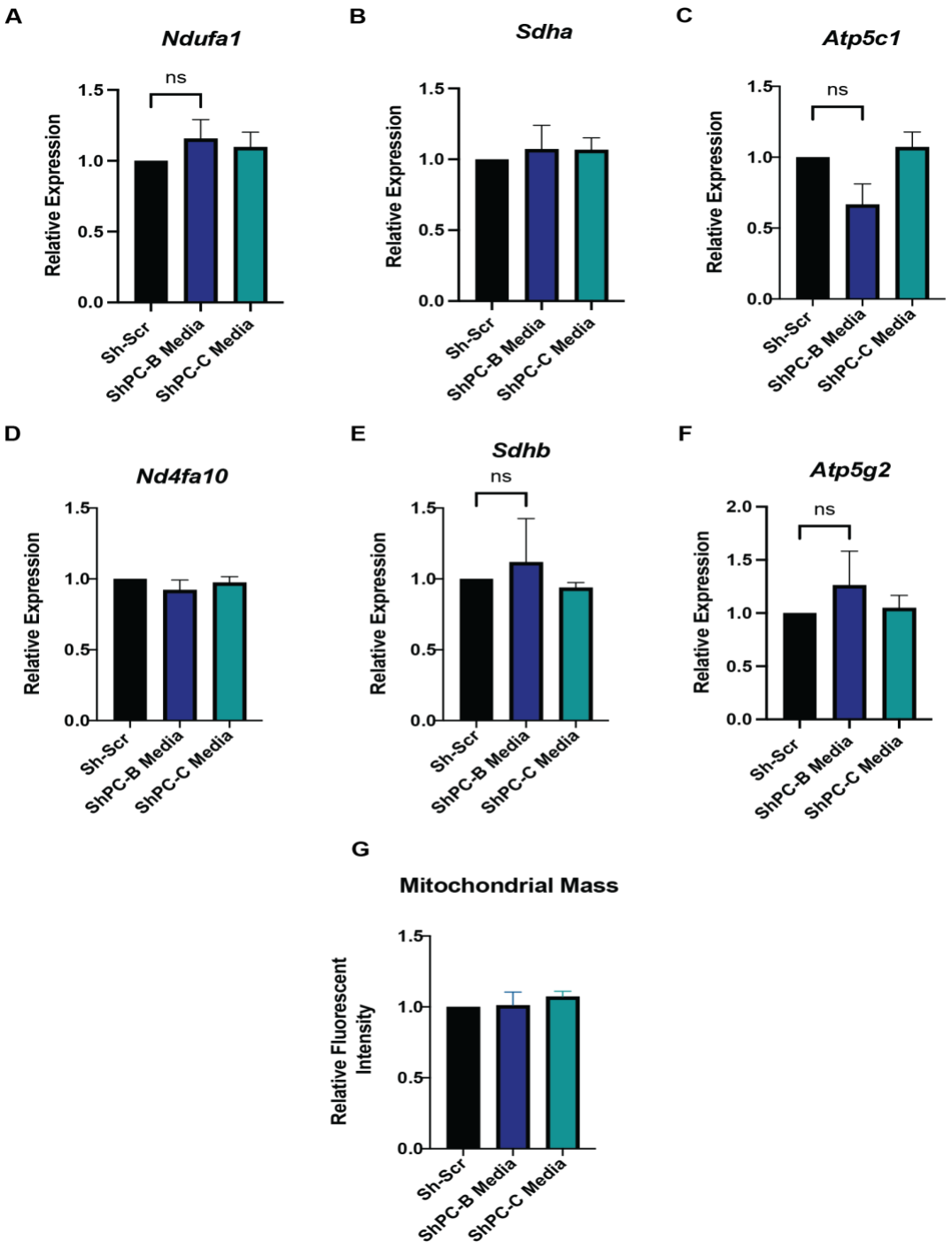

Figure 9: PC knockdown-mediated alterations to media composition does not drive the changes to mitochondrial ETC gene expression or mass. Relative gene expression of complex I, II, and V subunits in Sh-Scr cells seeded in the culture media of the ShPC-B or ShPC-C cell lines following a 48 hour incubation relative to controls cells seeded in their own culture media (n = 4 per group) (A-D). Relative fluorescent intensity following staining with MitoTracker Red diluted 1:2,000 in PBS (n = 4 per group) (E). All data presented with error bars representing means ± standard error of means (SEM).

CHAPTER 4: DISCUSSION AND FUTURE DIRECTIONS

PC is emerging as a key mediator of the metabolic reprogramming that mammary tumors evolve to utilize in supporting their growth, progression, and survival. Specifically, PC plays a critical role in breast cancer metastasis to the lung, supporting anaplerosis and the aerobic utilization of pyruvate required for adaptation to the oxygenated pulmonary microenvironment. At the primary site and non-pulmonary metastases, downregulation of PC likely supports aerobic glycolysis with enhanced carbon flux through LDH rather than anaplerotic entry into the mitochondrial TCA cycle; however, a complete understanding of the role of PC expression in primary tumor growth is currently lacking. In this study, a primary tumor model of TNBC was utilized to identify the metabolic and microenvironmental consequences of PC knockdown to further understand how PC expression can inform metabolic and immune-based therapies. In the pilot study utilizing a doxycycline-inducible ShRNA construct to target PC, an increase in primary tumor mass was observed when PC was suppressed by ~60% expression relative to control. This finding represents a novel relationship between PC expression and primary tumor growth, as previous literature utilizing pharmacological or genetic approaches to suppress PC activity have found either no growth effect or a deleterious growth effect in murine breast cancer models[62, 65].

To identify potential drivers of this pro-growth phenotype, the transcriptomes of excised tumor samples were analyzed utilizing GSEA. The Hallmarks gene set was chosen from the Molecular Signatures Database (MSigDB) as it contains 50 well defined gene sets aimed at identifying specific biological states with limited redundancy[107]. GSEA of transcriptomic data

offers valuable insight into phenotypic differences between groups, as analyzing changes to multiple genes along a pathway offers greater functional insight compared to curating a list of individual differentially expressed genes. All 8 immunological pathways included in the Hallmarks gene sets were found to be downregulated in PC knockdown tumors relative to control. In addition, 2 pathways involved in lipid metabolism, adipogenesis and fatty acid metabolism, were found to be downregulated by PC suppression. Although PC's role in lipid metabolism via replenishing oxaloacetate-derived carbons lost to citrate export for fatty acid synthesis has long been recognized[111], PC-mediated regulation of a broad array of pathways necessary for innate and adaptive anti-tumor immunity has not been described in the literature. The downregulation of these Hallmark gene sets including interferon alpha and gamma response, tumor necrosis factor-α (TNF-α) signaling, inflammatory response, and IL-2 signaling is characteristic of a "cold" or non-T-cell-inflamed TME[112]. Such TME's possess low levels of T cell infiltration, molecular signatures of dysregulated immune activation, and lower responses to immunotherapies[113, 114].

To investigate potential mediators of the diminished immune signaling observed in PC knockdown tumors, multiple constitutive PC knockdown cell lines utilizing ShRNAs were generated to manipulate lactate metabolism in the context of PC suppression. The connection of PC and lactate metabolism has a strong clinical basis, as individuals with inherited PC deficiency frequently present with severe lactic acidemia[115]. Indeed, lactate production in vitro was increased following PC knockdown of ~95% expression relative to control. In addition, PC knockdown cells showed an increased sensitivity to LDH inhibition, with increased cytotoxicity and a decrease in intracellular lactate concentrations at a dosage with minimal effect on control cells. The increased lactate production seen in inherited PC deficiency and our knockdown

model suggests that the flux of glucose-derived carbons through central carbon metabolism with limited PC activity cannot be fully supported by PDH-mediated incorporation of acetyl-coA into the TCA cycle or by other biosynthetic pathways that branch from glycolysis, thus requiring carbons to be shunted into lactate production. Increased flux through LDH is potentially advantageous in the setting of primary mammary tumors through multiple mechanisms, including: enhanced NAD^+ regeneration independent of the ETC to support the reductive nature of anabolism[14], acidifying the TME via increased co-transport of H^+ ions to create a pro-tumor environmental niche[116], and increasing extracellular lactate concentrations to drive immunosuppression of innate and adaptive immune populations[117].

As we hypothesized that the lactate-induced immunosuppression observed in our pilot study was driving the pro-growth effect of PC knockdown, we next investigated the potential to take advantage of the increased lactate production of PC knockdown tumors via a combination treatment approach utilizing FX11 and anti-PD1 therapy. Lactate metabolism inhibition is a promising area of metabolic-based cancer therapeutics, with clinical trials currently underway for the use of the MCT1 inhibitor AZD3965 in advanced solid tumors and diffuse large B cell lymphomas[118, 119]. In addition, LDH has been proposed as a prognostic marker for ICI therapies, with high pretreatment LDH levels correlating with shortened progression free survival in non-small cell lung cancer patients treated with ICIs[120]. Given lactates deleterious effects on $CD8^+$ T-cell activation and effector functions, high lactate in the TME is likely a major barrier to effective ICI response in solid tumors[121]. Indeed, therapeutic approaches combining lactate metabolism inhibition and ICIs have shown success in multiple murine cancer models[122-124]. We thus tested the hypothesis that reduced PC expression could be a marker for tumors that will see the greatest response to such a treatment approach. In

contrast to our pilot study, the ShPC-B cell line with a PC knockdown of ~95% expression resulted in reduced primary tumor mass relative to control. All three treatment groups, FX11, anti-PD1, and the combination, resulted in no changes to tumor mass in both control and PC knockdown conditions. The deleterious growth effect of the ShPC-B knockdown makes evaluation of the potential for this combination treatment approach difficult. Future investigations utilizing a more physiologically relevant downregulation of PC expression with a reduced magnitude of impact on tumor growth would better inform the utility of combining LDH inhibition and ICI in the context of PC suppression.

Given the dichotomous primary tumor results of the pilot and treatment study, we next utilized the ShPC-C cell line with a PC knockdown of 80% to monitor tumor growth without treatment and confirm if a pro-growth tumor phenotype is reproducible with PC knockdown M-Wnt cells. Indeed, the ShPC-C tumors recapitulated the pro-growth effect seen in the inducible ShPC model while ShPC-B tumors again showed reduced primary tumor mass. Thus, there appears to be heterogeneity in primary mammary tumor responses to PC modulation in both our models and the literature, with different cell lines and means of PC suppression having resulted in deleterious, neutral, or pro-growth effects. A possible contributor to this heterogeneity could be the degree of PC suppression, with PC knockdown of 95% relative expression or pharmacologic ablation of activity being detrimental to cellular metabolism and reducing tumor growth while PC suppression in the range of 60-80% may drive advantageous metabolic reprogramming and an immunosuppressed TME that enhances tumor growth. Additional mouse studies utilizing orthogonal means to suppress PC activity to varying degrees will be needed to delineate a potential correlation between PC expression and primary tumor growth. Further, this heterogeneity highlights a need for future investigations into the role of PC

in breast cancer to consider differences between PC suppression at the magnitude of intrinsic metabolic reprogramming in the tumor versus that seen following pharmacologic inhibition of the enzyme. Awareness of this distinction will be required to form and reproduce successful in vivo models for translational studies of therapeutic targets.

To elucidate potential mechanisms by which PC suppression can have variable effects on mammary tumor growth, we next investigated genomic and functional changes to the mitochondria of ShPC-B and ShPC-C cells in culture. Depletion of PC results in reduced glucose incorporation into TCA cycle intermediates downstream of oxaloacetate, including malate and citrate[64]. Hence, we tested the hypothesis that perturbations to the influx of carbons through the TCA cycle would result in reduced flux through the ETC and reduce the capacity of ShPC cells to undergo oxidative phosphorylation. Utilizing extracellular flux analysis and oxygen consumption rate as a proxy of ETC flux, PC suppression resulted in lowered basal and maximal OCR, with the ShPC-C cells experiencing a larger drop in basal and maximal OCR relative to ShPC-B. It is important to note that the media utilized in these assays contains hyper-physiological concentrations of glucose, pyruvate, and glutamine, though only glutamine is able to bypass the PC knockdown-mediated suppression of incorporation of 4-carbon units into the TCA cycle. Maximal OCR measurements following FCCP injections were taken to observe the capacity of the ETC without the constraint of complex V-mediated reductions to the electrochemical proton gradient. The difference between basal OCR and maximal OCR is thus a proxy for the level of flux control that complex V has on oxidative phosphorylation, which is a key regulatory mechanism of mitochondrial bioenergetics[125]. Reductions in maximal OCR following PC suppression revealed that the basal OCR in PC knockdown cells is not simply

limited by the flux control of the phosphorylation system when substrates are at basal concentrations, but that the capacity of the ETC is diminished.

To further probe the mechanisms by which PC suppression reduces both basal respiration and the capacity of the ETC, we utilized HRR of permeabilized cells following an established substrate-uncoupler-inhibitor titration (SUIT) protocol[126]. In contrast to extracellular flux analysis, HRR allows for highly sensitive measurements of oxygen consumption in a greater diversity of respiratory states at saturating concentrations of ETC substrates. Permeabilization of the plasma membrane results in the loss of endogenous substrates and thus allows for subsequent determination of complex level activity in multiple coupling states via sequential titrations of N-linked substrates, S-linked substrates, complex I and III inhibitors, and FCCP. The four coupling states achieved include: leak respiration measured prior to stimulation of complex V phosphorylation through absence of ADP, oxidative phosphorylation measured following addition of kinetically-saturating concentrations of ADP, inorganic phosphate, and fuel substrates, ETC capacity measured following titration of FCCP to collapse the electrochemical proton gradient, and residual oxygen consumption measured following loss of endogenous substrates after plasma membrane permeabilization. In contrast to the findings of extracellular flux analysis, ShPC-C cells had no changes to oxygen consumption in any of the examined respiratory states. ShPC-B cells had a significant increase in oxygen consumption relative to control cells in all conditions and relative to ShPC-C cells in the maximum flux state of $PGMS_E$ and S-linked respiration in the ET state, S_e. In addition, the flux control ratio (FCR) was consistent between both knockdown cell lines and control, indicating that PC suppression does not induce intrinsic ETC changes to complex-level flux control at saturating substrate concentrations.

The differential findings of oxygen consumption in extracellular flux analysis versus HRR is compatible with our hypothesis that PC suppression results in reduced flux of carbons through the TCA cycle, driving a reduction in oxidative phosphorylation. In HRR, N- and S-linked substrates are added to permeabilized cells at kinetically-saturating concentrations, with both malate and glutamine capable of directly entering the mitochondria from the extracellular space and generating reducing equivalents for the ETC independent of PC. Extracellular flux analysis measures OCR within intact cells that, while cultured in media with super-physiological concentrations of glutamine, glucose, and pyruvate, are still dependent on cellular substrate availability and utilization to fuel the ETC. Hence, HRR is a measure of solely mitochondrial metabolism independent of cellular substrate status whereas OCR in extracellular flux analysis is tightly controlled by cellular metabolism and PC activity. The increase in oxygen consumption of the ShPC-B cells in HRR suggests that PC knockdown can affect intrinsic ETC dynamics independent of substrate availability. The consistency in FCRs between knockdown and control cells indicates that the ShPC-B cells increased the efficiency of electron transport within their ETC without altering the relative contribution of the N- and S-linked substrates.

To further probe the differences in ETC alterations driven by the two PC knockdown lines, relative expression of multiple subunits of complexes I, II, and V was also determined. Interestingly, ShPC-B cells showed downregulation of a number of ETC complex subunits despite possessing higher oxygen flux relative to control cells as measured by HRR. ShPC-C cells possessed downregulation of a single subunit of complex V and to a significantly lower magnitude than seen in the ShPC-B cells. As the total surface area of inner mitochondrial membrane per cell could potentially explain these changes to gene expression, we utilized flow cytometry with cells stained for mitochondrial mass and found the ShPC-C cells to possess

greater mitochondrial mass relative to control. The ShPC-B cells showed no significant difference in mitochondrial mass, suggesting the downregulation in ETC subunits is not a function of mitochondrial size. As the profound expression changes in the ShPC-B cells were unexpected given the changes to oxygen consumption, we utilized an orthogonal approach to severely diminish PC activity to determine if the expression changes were related to the degree of PC knockdown and not an artifact of the lentivirus-transduced cell line. Utilizing Si-RNA transfection to achieve a PC knockdown of 92% expression, the gene expression changes seen in the ShPC-B line were largely recapitulated with downregulation of the selected subunits in complexes I, II, and V. The similar results from the orthogonal means of PC knockdown suggests that PC knockdown of greater than 90% results in distinct changes to the gene expression of ETC subunits.

As the varying degree of PC knockdown could also affect the concentrations of metabolites in the extracellular space, ETC gene expression values were analyzed following the culture of Sh-Scr cells in media conditioned by 48 hours of growth with the knockdown cell lines. These comparisons were made to distinguish if any changes to ETC gene expression or mitochondrial mass were mediated specifically by intrinsic PC activity or indirect metabolic perturbations to substrate availability. None of the genes analyzed nor mitochondrial mass were found to be modulated by the different medias.

Importantly, screening of a limited number of ETC subunit expression values is insufficient to understand the totality of effect that changes to the ETC have on the function of the mitochondria. Control over the flux of electrons and phosphorylation of ATP is widely shared among the subunits of each complex, with no one enzyme being rate-limiting and the distribution of control altering as environmental conditions change[127]. Further, the complexes

of the ETC are encoded by both nuclear and mitochondrial genes, with complex I composed of 38 nuclear-encoded subunits and 7 mitochondrial-encoded subunits. Thus, these comparisons of only a few nuclear-encoded mitochondrial genes from each complex provides evidence that the degree of PC knockdown may determine distinct changes to the ETC expression programming. However, extrapolation of the ultimate bioenergetic consequences of these changes would be misguided. A potential explanation for the lack of changes to ETC gene expression in the ShPC-C cells could be made from the observed increase in mitochondrial mass. It is possible that these cells do experience downregulation of the subunits examined if normalized to total mitochondrial mass, but that a concomitant increase in mitochondrial size via mitochondrial biogenesis regulation makes the expression data appear neutral. Future investigations analyzing a greater number of both nuclear- and mitochondrial-encoded genes and their protein content, normalized to mitochondrial mass, would allow greater insight into the functional consequences of PC knockdown-induced changes to the ETC.

Future Directions

Taken together, this project reveals important nuance to the effects of PC knockdown on primary mammary tumor growth and metabolic reprogramming. The differential findings of the ShPC-C line resulting in enhanced tumor growth and immunosuppression versus the ShPC-B line reducing tumor growth highlights the need for further investigation into the mechanisms driving such a dichotomous role for PC at the primary site. Future mouse studies utilizing orthogonal means to suppress PC activity to the level of the ShPC-B knockdown via genetic or pharmacological approaches would be beneficial in delineating if there exists a threshold of PC activity that tumors require before their growth is adversely affected. In addition, re-attempting the combination treatment approach of FX11 and anti-PD1 therapy with PC

knockdown cell lines that enhance tumor growth would better inform the utility of targeting the enhanced lactate production and immunosuppression induced by certain degrees of PC suppression. Together, these future directions may reveal two separate approaches by which to use PC expression to inform adjuvant therapeutic options: 1) In tumors with enhanced PC expression and hence increased risk for metastatic spread to the lung, targeting of PC directly via a small molecule inhibitor could diminish both primary tumor growth and metastatic spread. 2) Tumors with reduced PC expression may be especially sensitive to a combination treatment approach of FX11 and anti-PD1 relative to other mammary tumors with a decreased reliance on lactate metabolism.

In addition to further investigations into the in vivo therapeutic targets of PC knockdown cell lines, additional in vitro studies are needed to better understand the metabolic reprogramming that underlies the enhanced lactate production and reduced oxidative phosphorylation following PC suppression. Though the HRR and extracellular flux analysis results are congruent with the hypothesis that decreased anaplerotic refilling of TCA cycle intermediates is driving these effects, metabolomic analysis is needed to directly recognize any changes to the concentrations of TCA cycle substrates. Rescue experiments utilizing cell-permeable precursors of TCA cycle intermediates such as dimethyl α-ketoglutarate aimed at returning basal OCR to control levels in extracellular flux analysis would also be helpful for such ends. Metabolomic analysis would also help to identify other pathways that are likely affected by PC suppression, including fatty acid metabolism and amino acid synthesis pathways such as those for serine, glycine, and aspartate. Such pathways may underlie the dichotomous primary tumor growth effects seen following PC knockdown, as the differences in mitochondrial function and gene expression examined in this study are insufficient to explain such findings.

CHAPTER 5: CONCLUSIONS

PC's role in the metabolic reprogramming that drives breast cancer growth and metastatic potential is a growing area of interest. Though enhanced PC activity is required for pulmonary metastasis in mammary tumor models, the impact of varying degrees of PC expression at the primary tumor is not well understood. This gap in knowledge must be reconciled prior to effective targeting of PC in cancer therapeutics, where targeted therapies based on metabolic signatures hold promise in improving current standards of care for TNBC in particular. This study thus aimed to assess the impact of PC suppression on primary mammary tumor growth and if the resulting metabolic reprogramming could inform the use of metabolic therapies as adjuvants to immune-checkpoint inhibition.

Taken together, this project provides insight into a variable role of PC in primary mammary tumor growth while identifying important alterations to central carbon and mitochondrial metabolism following PC suppression. Namely, PC knockdown of 60-80% expression resulted in enhanced primary tumor growth and a transcriptomic signature of immunosuppression, while PC knockdown of 95% expression was deleterious to tumor growth. In vitro assays further revealed reduced PC-mediated anaplerosis to increase lactate export and render cells more sensitive to LDH inhibition. Extracellular flux analysis found both PC knockdown lines to have reduced OCR relative to control, likely as a function of reduced TCA cycle intermediates. HRR and ETC gene expression analysis found important mitochondrial differences between the two knockdowns, though these differences are not sufficient to attempt to explain the dichotomous effects on primary mammary tumor growth. These findings should be

considered for future investigations into identifying circumstances in which targeting PC or its downstream metabolic effectors may be beneficial in the treatment of TNBC.

REFERENCES

1. Sung, H., et al., *Global cancer statistics 2020: GLOBOCAN estimates of incidence and mortality worldwide for 36 cancers in 185 countries.* CA: a cancer journal for clinicians, 2021. **71**(3): p. 209-249.

2. Siegel, R.L., et al., *Cancer statistics, 2021.* CA: a cancer journal for clinicians, 2021. **71**(1): p. 7-33.

3. Kiely, B.E., et al., *How long have I got? Estimating typical, best-case, and worst-case scenarios for patients starting first-line chemotherapy for metastatic breast cancer: a systematic review of recent randomized trials.* Journal of Clinical Oncology, 2011. **29**(4): p. 456-463.

4. Yin, L., et al., *Triple-negative breast cancer molecular subtyping and treatment progress.* Breast Cancer Research, 2020. **22**(1): p. 1-13.

5. Ismail-Khan, R. and M.M. Bui, *A review of triple-negative breast cancer.* Cancer Control, 2010. **17**(3): p. 173-176.

6. Gluz, O., et al., *Triple-negative breast cancer—current status and future directions.* Annals of Oncology, 2009. **20**(12): p. 1913-1927.

7. Dawood, S., *Triple-negative breast cancer.* Drugs, 2010. **70**(17): p. 2247-2258.

8. Warburg, O., *On the origin of cancer cells.* Science, 1956. **123**(3191): p. 309-314.

9. Warburg, O., *On respiratory impairment in cancer cells.* Science, 1956. **124**(3215): p. 269-270.

10. Lunt, S.Y. and M.G. Vander Heiden, *Aerobic glycolysis: meeting the metabolic requirements of cell proliferation.* Annual review of cell and developmental biology, 2011. **27**: p. 441-464.

11. Porporato, P.E., et al., *Mitochondrial metabolism and cancer.* Cell research, 2018. **28**(3): p. 265-280.

12. Zu, X.L. and M. Guppy, *Cancer metabolism: facts, fantasy, and fiction.* Biochemical and biophysical research communications, 2004. **313**(3): p. 459-465.

13. Liberti, M.V. and J.W. Locasale, *The Warburg effect: how does it benefit cancer cells?* Trends in biochemical sciences, 2016. **41**(3): p. 211-218.

14. Luengo, A., et al., *Increased demand for NAD+ relative to ATP drives aerobic glycolysis.* Molecular cell, 2021. **81**(4): p. 691-707. e6.

15. Schuster, S., et al., *Mathematical models for explaining the Warburg effect: a review focussed on ATP and biomass production.* Biochemical Society Transactions, 2015. **43**(6): p. 1187-1194.

16. Hanahan, D. and R.A. Weinberg, *The hallmarks of cancer.* cell, 2000. **100**(1): p. 57-70.

17. Pavlova, N.N. and C.B. Thompson, *The emerging hallmarks of cancer metabolism.* Cell metabolism, 2016. **23**(1): p. 27-47.

18. DeBerardinis, R.J. and N.S. Chandel, *Fundamentals of cancer metabolism.* Science advances, 2016. **2**(5): p. e1600200.

19. Tan, A.S., et al., *Mitochondrial genome acquisition restores respiratory function and tumorigenic potential of cancer cells without mitochondrial DNA.* Cell metabolism, 2015. **21**(1): p. 81-94.

20. Idelchik, M.d.P.S., et al. *Mitochondrial ROS control of cancer*. in *Seminars in cancer biology*. 2017. Elsevier.

21. Martínez-Reyes, I., et al., *Mitochondrial ubiquinol oxidation is necessary for tumour growth.* Nature, 2020. **585**(7824): p. 288-292.

22. Liu, X., et al., *Induction of apoptotic program in cell-free extracts: requirement for dATP and cytochrome c.* Cell, 1996. **86**(1): p. 147-157.

23. Martínez-Reyes, I. and N.S. Chandel, *Mitochondrial one-carbon metabolism maintains redox balance during hypoxia.* Cancer discovery, 2014. **4**(12): p. 1371-1373.

24. Letouzé, E., et al., *SDH mutations establish a hypermethylator phenotype in paraganglioma.* Cancer cell, 2013. **23**(6): p. 739-752.

25. Sciacovelli, M., et al., *Fumarate is an epigenetic modifier that elicits epithelial-to-mesenchymal transition.* Nature, 2016. **537**(7621): p. 544-547.

26. Yan, H., et al., *IDH1 and IDH2 mutations in gliomas.* New England journal of medicine, 2009. **360**(8): p. 765-773.

27. Whiteside, T., *The tumor microenvironment and its role in promoting tumor growth.* Oncogene, 2008. **27**(45): p. 5904-5912.

28. Joyce, J.A., *Therapeutic targeting of the tumor microenvironment.* Cancer cell, 2005. **7**(6): p. 513-520.

29. Mbeunkui, F. and D.J. Johann, *Cancer and the tumor microenvironment: a review of an essential relationship.* Cancer chemotherapy and pharmacology, 2009. **63**(4): p. 571-582.

30. Mao, Y., et al., *Stromal cells in tumor microenvironment and breast cancer.* Cancer and Metastasis Reviews, 2013. **32**(1): p. 303-315.

31. Eiro, N., et al., *Cancer-associated fibroblasts affect breast cancer cell gene expression, invasion and angiogenesis.* Cellular Oncology, 2018. **41**(4): p. 369-378.

32. Migneco, G., et al., *Glycolytic cancer associated fibroblasts promote breast cancer tumor growth, without a measurable increase in angiogenesis: evidence for stromal-epithelial metabolic coupling.* Cell cycle, 2010. **9**(12): p. 2412-2422.

33. Costa, A., et al., *Fibroblast heterogeneity and immunosuppressive environment in human breast cancer.* Cancer cell, 2018. **33**(3): p. 463-479. e10.

34. Pavlides, S., et al., *The reverse Warburg effect: aerobic glycolysis in cancer associated fibroblasts and the tumor stroma.* Cell cycle, 2009. **8**(23): p. 3984-4001.

35. Witkiewicz, A.K., et al., *Using the "reverse Warburg effect" to identify high-risk breast cancer patients: stromal MCT4 predicts poor clinical outcome in triple-negative breast cancers.* Cell cycle, 2012. **11**(6): p. 1108-1117.

36. Fu, Y., et al., *The reverse Warburg effect is likely to be an Achilles' heel of cancer that can be exploited for cancer therapy.* Oncotarget, 2017. **8**(34): p. 57813.

37. Vaupel, P. and A. Mayer, *Hypoxia in cancer: significance and impact on clinical outcome.* Cancer and Metastasis Reviews, 2007. **26**(2): p. 225-239.

38. Nakajima, E.C. and B. Van Houten, *Metabolic symbiosis in cancer: refocusing the Warburg lens.* Molecular carcinogenesis, 2013. **52**(5): p. 329-337.

39. Ohshima, K. and E. Morii, *Metabolic reprogramming of cancer cells during tumor progression and metastasis.* Metabolites, 2021. **11**(1): p. 28.

40. Pantel, K. and R.H. Brakenhoff, *Dissecting the metastatic cascade.* Nature reviews cancer, 2004. **4**(6): p. 448-456.

41. Baccelli, I., et al., *Identification of a population of blood circulating tumor cells from breast cancer patients that initiates metastasis in a xenograft assay.* Nature biotechnology, 2013. **31**(6): p. 539-544.

42. Luzzi, K.J., et al., *Multistep nature of metastatic inefficiency: dormancy of solitary cells after successful extravasation and limited survival of early micrometastases.* The American journal of pathology, 1998. **153**(3): p. 865-873.

43. Bergers, G. and S.-M. Fendt, *The metabolism of cancer cells during metastasis.* Nature Reviews Cancer, 2021. **21**(3): p. 162-180.

44. Gaude, E. and C. Frezza, *Tissue-specific and convergent metabolic transformation of cancer correlates with metastatic potential and patient survival.* Nature communications, 2016. **7**(1): p. 1-9.

45. Lu, J., M. Tan, and Q. Cai, *The Warburg effect in tumor progression: mitochondrial oxidative metabolism as an anti-metastasis mechanism.* Cancer letters, 2015. **356**(2): p. 156-164.

46. Dupuy, F., et al., *PDK1-dependent metabolic reprogramming dictates metastatic potential in breast cancer.* Cell metabolism, 2015. **22**(4): p. 577-589.

47. Kim, H.M., W.H. Jung, and J.S. Koo, *Site-specific metabolic phenotypes in metastatic breast cancer.* Journal of translational medicine, 2014. **12**(1): p. 1-17.

48. Simões, R.V., et al., *Metabolic plasticity of metastatic breast cancer cells: adaptation to changes in the microenvironment.* Neoplasia, 2015. **17**(8): p. 671-684.

49. Li, L., et al., *miR-30a-5p suppresses breast tumor growth and metastasis through inhibition of LDHA-mediated Warburg effect.* Cancer letters, 2017. **400**: p. 89-98.

50. Andrzejewski, S., et al., *PGC-1α promotes breast cancer metastasis and confers bioenergetic flexibility against metabolic drugs.* Cell metabolism, 2017. **26**(5): p. 778-787. e5.

51. Li, A.M., et al., *Metabolic profiling reveals a dependency of human metastatic breast cancer on mitochondrial serine and one-carbon unit metabolism.* Molecular Cancer Research, 2020. **18**(4): p. 599-611.

52. Ahn, C.S. and C.M. Metallo, *Mitochondria as biosynthetic factories for cancer proliferation.* Cancer & metabolism, 2015. **3**(1): p. 1-10.

53. Owen, O.E., S.C. Kalhan, and R.W. Hanson, *The key role of anaplerosis and cataplerosis for citric acid cycle function.* Journal of Biological Chemistry, 2002. **277**(34): p. 30409-30412.

54. DeBerardinis, R.J., et al., *Beyond aerobic glycolysis: transformed cells can engage in glutamine metabolism that exceeds the requirement for protein and nucleotide synthesis.* Proceedings of the National Academy of Sciences, 2007. **104**(49): p. 19345-19350.

55. Lao-On, U., P.V. Attwood, and S. Jitrapakdee, *Roles of pyruvate carboxylase in human diseases: from diabetes to cancers and infection.* Journal of Molecular Medicine, 2018. **96**(3): p. 237-247.

56. Jitrapakdee, S., A. Vidal-Puig, and J. Wallace, *Anaplerotic roles of pyruvate carboxylase in mammalian tissues.* Cellular and Molecular Life Sciences CMLS, 2006. **63**(7): p. 843-854.

57. Kiesel, V.A., et al., *Pyruvate carboxylase and cancer progression.* Cancer & Metabolism, 2021. **9**(1): p. 1-13.

58. Portais, J., et al., *Glucose and glutamine metabolism in C6 glioma cells studied by carbon 13 NMR.* Biochimie, 1996. **78**(3): p. 155-164.

59. Cheng, T., et al., *Pyruvate carboxylase is required for glutamine-independent growth of tumor cells.* Proceedings of the National Academy of Sciences, 2011. **108**(21): p. 8674-8679.

60. Cetinbas, N.M., et al., *Glucose-dependent anaplerosis in cancer cells is required for cellular redox balance in the absence of glutamine.* Scientific reports, 2016. **6**(1): p. 1-12.

61. Cardaci, S., et al., *Pyruvate carboxylation enables growth of SDH-deficient cells by supporting aspartate biosynthesis.* Nature cell biology, 2015. **17**(10): p. 1317-1326.

62. Shinde, A., et al., *Pyruvate carboxylase supports the pulmonary tropism of metastatic breast cancer.* Breast Cancer Research, 2018. **20**(1): p. 1-12.

63. Phannasil, P., et al., *Pyruvate carboxylase is up-regulated in breast cancer and essential to support growth and invasion of MDA-MB-231 cells.* PloS one, 2015. **10**(6): p. e0129848.

64. Phannasil, P., et al., *Mass spectrometry analysis shows the biosynthetic pathways supported by pyruvate carboxylase in highly invasive breast cancer cells.* Biochimica et Biophysica Acta (BBA)-Molecular Basis of Disease, 2017. **1863**(2): p. 537-551.

65. Lin, Q., et al., *Targeting pyruvate carboxylase by a small molecule suppresses breast cancer progression.* Advanced Science, 2020. **7**(9): p. 1903483.

66. Pinweha, P., et al., *MicroRNA-143-3p targets pyruvate carboxylase expression and controls proliferation and migration of MDA-MB-231 cells.* Archives of biochemistry and biophysics, 2019. **677**: p. 108169.

67. Wilmanski, T., et al., *Inhibition of pyruvate carboxylase by 1α, 25-dihydroxyvitamin D promotes oxidative stress in early breast cancer progression.* Cancer letters, 2017. **411**: p. 171-181.

68. Wilmanski, T., et al., *1α, 25-dihydroxyvitamin D inhibits de novo fatty acid synthesis and lipid accumulation in metastatic breast cancer cells through down-regulation of pyruvate carboxylase.* The Journal of nutritional biochemistry, 2017. **40**: p. 194-200.

69. Kennedy, L., et al., *Role of glutathione in cancer: From mechanisms to therapies.* Biomolecules, 2020. **10**(10): p. 1429.

70. Murai, S., et al., *Inhibition of malic enzyme 1 disrupts cellular metabolism and leads to vulnerability in cancer cells in glucose-restricted conditions.* Oncogenesis, 2017. **6**(5): p. e329-e329.

71. Perry, R.R., et al., *Glutathione levels and variability in breast tumors and normal tissue.* Cancer, 1993. **72**(3): p. 783-787.

72. Nath, A. and C. Chan, *Genetic alterations in fatty acid transport and metabolism genes are associated with metastatic progression and poor prognosis of human cancers.* Scientific reports, 2016. **6**(1): p. 1-13.

73. Christen, S., et al., *Breast cancer-derived lung metastases show increased pyruvate carboxylase-dependent anaplerosis.* Cell reports, 2016. **17**(3): p. 837-848.

74. Sellers, K., et al., *Pyruvate carboxylase is critical for non–small-cell lung cancer proliferation.* The Journal of clinical investigation, 2015. **125**(2): p. 687-698.

75. Graves, E.E., A. Maity, and Q.-T. Le. *The tumor microenvironment in non–small-cell lung cancer*. in *Seminars in radiation oncology*. 2010. Elsevier.

76. Kim, J.-w., et al., *HIF-1-mediated expression of pyruvate dehydrogenase kinase: a metabolic switch required for cellular adaptation to hypoxia.* Cell metabolism, 2006. **3**(3): p. 177-185.

77. DEVIVO, D.C., et al., *The clinical and biochemical implications of pyruvate carboxylase deficiency.* The Journal of Clinical Endocrinology & Metabolism, 1977. **45**(6): p. 1281-1296.

78. Vonderheide, R.H., S.M. Domchek, and A.S. Clark, *Immunotherapy for breast cancer: what are we missing?* 2017, AACR. p. 2640-2646.

79. Gajewski, T.F., et al., *Cancer immunotherapy strategies based on overcoming barriers within the tumor microenvironment.* Current opinion in immunology, 2013. **25**(2): p. 268-276.

80. Sukumar, M., R. Roychoudhuri, and N.P. Restifo, *Nutrient competition: a new axis of tumor immunosuppression.* Cell, 2015. **162**(6): p. 1206-1208.

81. Wang, R. and D.R. Green, *Metabolic reprogramming and metabolic dependency in T cells.* Immunological reviews, 2012. **249**(1): p. 14-26.

82. Kelly, B. and L.A. O'neill, *Metabolic reprogramming in macrophages and dendritic cells in innate immunity.* Cell research, 2015. **25**(7): p. 771-784.

83. Finlay, D.K., *Metabolic regulation of natural killer cells.* Biochemical Society transactions, 2015. **43**(4): p. 758-762.

84. Chang, C.-H., et al., *Metabolic competition in the tumor microenvironment is a driver of cancer progression.* Cell, 2015. **162**(6): p. 1229-1241.

85. MacIver, N.J., R.D. Michalek, and J.C. Rathmell, *Metabolic regulation of T lymphocytes.* Annual review of immunology, 2013. **31**: p. 259-283.

86. Michalek, R.D., et al., *Cutting edge: distinct glycolytic and lipid oxidative metabolic programs are essential for effector and regulatory CD4+ T cell subsets.* The Journal of Immunology, 2011. **186**(6): p. 3299-3303.

87. Bates, G.J., et al., *Quantification of regulatory T cells enables the identification of high-risk breast cancer patients and those at risk of late relapse.* Journal of clinical oncology, 2006. **24**(34): p. 5373-5380.

88. Harmon, C., C. O'Farrelly, and M.W. Robinson, *The immune consequences of lactate in the tumor microenvironment*, in *Tumor Microenvironment*. 2020, Springer. p. 113-124.

89. Brizel, D.M., et al., *Elevated tumor lactate concentrations predict for an increased risk of metastases in head-and-neck cancer.* International Journal of Radiation Oncology* Biology* Physics, 2001. **51**(2): p. 349-353.

90. Holm, E., et al., *Substrate balances across colonic carcinomas in humans.* Cancer research, 1995. **55**(6): p. 1373-1378.

91. Haas, R., et al., *Lactate regulates metabolic and pro-inflammatory circuits in control of T cell migration and effector functions.* PLoS biology, 2015. **13**(7): p. e1002202.

92. Raychaudhuri, D., et al., *Lactate induces pro-tumor reprogramming in intratumoral plasmacytoid dendritic cells.* Frontiers in immunology, 2019. **10**: p. 1878.

93. Mu, X., et al., *Tumor-derived lactate induces M2 macrophage polarization via the activation of the ERK/STAT3 signaling pathway in breast cancer.* Cell Cycle, 2018. **17**(4): p. 428-438.

94. Brand, A., et al., *LDHA-associated lactic acid production blunts tumor immunosurveillance by T and NK cells.* Cell metabolism, 2016. **24**(5): p. 657-671.

95. Kato, Y., et al., *Acidic extracellular microenvironment and cancer.* Cancer cell international, 2013. **13**(1): p. 1-8.

96. Calcinotto, A., et al., *Modulation of microenvironment acidity reverses anergy in human and murine tumor-infiltrating T lymphocytes.* Cancer research, 2012. **72**(11): p. 2746-2756.

97. Johnston, R.J., et al., *VISTA is an acidic pH-selective ligand for PSGL-1.* Nature, 2019. **574**(7779): p. 565-570.

98. Fischer, K., et al., *Inhibitory effect of tumor cell–derived lactic acid on human T cells.* Blood, 2007. **109**(9): p. 3812-3819.

99. Walenta, S., et al., *High lactate levels predict likelihood of metastases, tumor recurrence, and restricted patient survival in human cervical cancers.* Cancer research, 2000. **60**(4): p. 916-921.

100. Cascone, T., et al., *Increased tumor glycolysis characterizes immune resistance to adoptive T cell therapy.* Cell metabolism, 2018. **27**(5): p. 977-987. e4.

101. Beloueche-Babari, M., et al., *MCT1 inhibitor AZD3965 increases mitochondrial metabolism, facilitating combination therapy and noninvasive magnetic resonance spectroscopy.* Cancer research, 2017. **77**(21): p. 5913-5924.

102. Sharpe, A.H. and K.E. Pauken, *The diverse functions of the PD1 inhibitory pathway.* Nature Reviews Immunology, 2018. **18**(3): p. 153-167.

103. Pauken, K.E. and E.J. Wherry, *Overcoming T cell exhaustion in infection and cancer*. Trends in immunology, 2015. **36**(4): p. 265-276.

104. Patsoukis, N., et al., *Revisiting the PD-1 pathway.* Science Advances, 2020. **6**(38): p. eabd2712.

105. Patsoukis, N., et al., *PD-1 alters T-cell metabolic reprogramming by inhibiting glycolysis and promoting lipolysis and fatty acid oxidation.* Nature communications, 2015. **6**(1): p. 1-13.

106. Arasanz, H., et al., *PD1 signal transduction pathways in T cells.* Oncotarget, 2017. **8**(31): p. 51936.

107. Liberzon, A., et al., *The molecular signatures database hallmark gene set collection.* Cell systems, 2015. **1**(6): p. 417-425.

108. Subramanian, A., et al., *Gene set enrichment analysis: a knowledge-based approach for interpreting genome-wide expression profiles.* Proceedings of the National Academy of Sciences, 2005. **102**(43): p. 15545-15550.

109. Wang, X., et al., *PrimerBank: a PCR primer database for quantitative gene expression analysis, 2012 update.* Nucleic acids research, 2012. **40**(D1): p. D1144-D1149.

110. Livak, K.J. and T.D. Schmittgen, *Analysis of relative gene expression data using real-time quantitative PCR and the 2− ΔΔCT method.* methods, 2001. **25**(4): p. 402-408.

111. Mackall, J.C. and M.D. Lane, *Role of pyruvate carboxylase in fatty acid synthesis: alterations during preadipocyte differentiation.* Biochemical and Biophysical Research Communications, 1977. **79**(3): p. 720-725.

112. Gajewski, T.F. *The next hurdle in cancer immunotherapy: overcoming the non–T-cell–inflamed tumor microenvironment*. in *Seminars in oncology*. 2015. Elsevier.

113. Duan, Q., et al., *Turning cold into hot: firing up the tumor microenvironment.* Trends in cancer, 2020. **6**(7): p. 605-618.

114. Zemek, R.M., et al., *Sensitization to immune checkpoint blockade through activation of a STAT1/NK axis in the tumor microenvironment.* Science translational medicine, 2019. **11**(501): p. eaav7816.

115. Marin-Valencia, I., C.R. Roe, and J.M. Pascual, *Pyruvate carboxylase deficiency: mechanisms, mimics and anaplerosis.* Molecular genetics and metabolism, 2010. **101**(1): p. 9-17.

116. Boedtkjer, E. and S.F. Pedersen, *The acidic tumor microenvironment as a driver of cancer.* Annual review of physiology, 2020. **82**: p. 103-126.

117. Harmon, C., C. O'Farrelly, and M.W. Robinson, *The immune consequences of lactate in the tumor microenvironment.* Tumor Microenvironment, 2020: p. 113-124.

118. Doherty, J.R. and J.L. Cleveland, *Targeting lactate metabolism for cancer therapeutics.* The Journal of clinical investigation, 2013. **123**(9): p. 3685-3692.

119. Halford, S.E., et al., *A first-in-human first-in-class (FIC) trial of the monocarboxylate transporter 1 (MCT1) inhibitor AZD3965 in patients with advanced solid tumours*. 2017, American Society of Clinical Oncology.

120. Zhang, Z., et al., *Pretreatment lactate dehydrogenase may predict outcome of advanced non small-cell lung cancer patients treated with immune checkpoint inhibitors: A meta-analysis.* Cancer medicine, 2019. **8**(4): p. 1467-1473.

121. Hayes, C., et al., *The oncogenic and clinical implications of lactate induced immunosuppression in the tumour microenvironment.* Cancer Letters, 2021. **500**: p. 75-86.

122. Gong, Y., et al., *Metabolic-pathway-based subtyping of triple-negative breast cancer reveals potential therapeutic targets.* Cell metabolism, 2021. **33**(1): p. 51-64. e9.

123. Huang, T., et al., *Tumor-Targeted Inhibition of Monocarboxylate Transporter 1 Improves T-Cell Immunotherapy of Solid Tumors.* Advanced Healthcare Materials, 2021. **10**(4): p. 2000549.

124. Daneshmandi, S., B. Wegiel, and P. Seth, *Blockade of lactate dehydrogenase-A (LDH-A) improves efficacy of anti-programmed cell death-1 (PD-1) therapy in melanoma.* Cancers, 2019. **11**(4): p. 450.

125. Das, A.M., *Regulation of the mitochondrial ATP-synthase in health and disease.* Molecular genetics and metabolism, 2003. **79**(2): p. 71-82.

126. Pesta, D. and E. Gnaiger, *High-Resolution Respirometry: OXPHOS Protocols for Human Cells and Permeabilized Fibers from Small Biopsies of Human Muscle*, in *Mitochondrial Bioenergetics: Methods and Protocols*, C.M. Palmeira and A.J. Moreno, Editors. 2012, Humana Press: Totowa, NJ. p. 25-58.

127. Brand, M. and D. Nicholls, *Assessing mitochondrial dysfunction in cells The Biochemical journal 435: 297–312 doi: 10.1042.* BJ20110162, 2011.